European Journal of Soil Science

WILEY

RESEARCH ARTICLE OPEN ACCESS

Modelling Long-Term Effects of Soil Compaction on Crop Yield, Soil Organic Carbon Stocks and Nitrogen Losses From Soil

Alejandro Romero-Ruiz[1] | Lorena Chagas Torres[2] | Mathieu Lamandé[3] | Michael Kuhwald[3,4,5] | Thomas Keller[1,2]

[1]Department of Agroecology and Environment, Agroscope, Zürich, Switzerland | [2]Department of Soil and Environment, Swedish University of Agricultural Sciences, Uppsala, Sweden | [3]Department of Agroecology - Soil Physics and Hydropedology, Aarhus University, Aarhus, Denmark | [4]Department of Geography, Landscape Ecology and Geoinformation Science, Kiel University, Kiel, Germany | [5]Thünen Institute of Agricultural Technology, Braunschweig, Germany

Correspondence: Alejandro Romero-Ruiz (alejandro.romero-ruiz@outlook.com)

Received: 7 April 2025 | **Revised:** 20 February 2026 | **Accepted:** 17 March 2026

Keywords: agroecosystem modelling | crop yield | nitrate leaching | nitrous oxide emissions | soil carbon stocks | soil degradation

ABSTRACT

Soil compaction is an increasing environmental threat due to agricultural intensification. Compaction negatively affects both agricultural production and key soil environmental functions. In this study, we developed a novel soil-compaction-agroecosystem modelling framework to systematically assess the consequences of soil compaction on crop yield, soil organic carbon stocks, nitrous oxide emissions and nitrogen leaching in the long-term. The modelling was done for different soil textures, different climatic conditions and different soil structure recovery rates, each of them tested comprising three cases. We compared simulations with data from field observations compiled from the literature. The modelling results reproduced most trends reported in the literature. Comparing compacted vs. non-compacted simulations, the accumulated effects over a 20 year-long period caused by a single wheeling event (two axle passes with 8 Mg wheel load) on a loamy soil without soil structure recovery and weather conditions of central Europe were estimated to account for an accumulated loss of about 21 Mg ha^{-1} in cereal grain yield, a decrease of nearly 1.8% in soil organic carbon (corresponding to a loss of about 1 Mg ha^{-1}), an increase of 130% in nitrous oxide emissions (about 0.5 kg ha^{-1} annual increase) and an increase of 15% in nitrate leaching (annual increase of approximately 8 kg ha^{-1}). This work offers a novel approach for accounting for effects of compaction on interacting soil processes and enables the quantification of long-term adverse impacts of soil compaction on key soil ecosystem services across diverse pedoclimatic conditions, thereby providing a scientific basis for the design of effective mitigation strategies.

1 | Introduction

Soil compaction is a major environmental issue, affecting soils in all terrestrial ecosystems and climates (Chamen et al. 2015; Hamza and Anderson 2005; Nawaz et al. 2013). Soil compaction is caused by construction, military, agricultural and forestry operations involving heavy vehicles and due to grazing animals trampling on the soil under mechanically vulnerable conditions. Almost three decades ago, Oldeman (1992) estimated that 68 Mha of agricultural lands are compacted worldwide and two decades ago Steinfeld et al. (2006) estimated that 20% of the world's grassland is degraded by overgrazing and compaction. The size and weight of vehicles and the intensity of grazing have continued to increase in recent years in response to food demands of a growing population (Van Dijk et al. 2021). This, combined with the slow recovery rates of soil structure following compaction, suggests that soil compaction levels and extent have increased during recent years (Keller and Or 2022).

Highlights

- A literature synthesis was conducted on compaction-induced crop yield, carbon and nitrogen losses
- Compaction may increase or decrease organic carbon stocks and nitrate leaching.
- A novel soil-compaction-agroecosystem model was developed to study compaction impacts on soil functions.
- Modelled compaction impacts on soil services are highly sensitive to soil type and climate.

Compaction induces changes in soil pore structure, often implying reduction and disruption of soil macroporosity that lead to significant reductions in soil water and gas transport properties (Berisso et al. 2012) and increases soil mechanical resistance to root penetration (Colombi et al. 2018). This has a negative impact on soil physical and biological processes such as water infiltration, oxygen diffusion, root growth (Rabot et al. 2018) and carbon and nutrient cycling (Tubeileh et al. 2003). The reduction in soil water and gas transport properties (e.g., hydraulic conductivity, air permeability, gas diffusivity) may promote anaerobic conditions within the soil, enhancing nitrous oxide emissions (Pulido-Moncada et al. 2022). In addition, root penetration is hampered due to an increase in mechanical resistance of the soil, which limits root access to nutrients and water and may promote nutrient leaching. Such limiting plant growing conditions produce a decrease in soil productivity, manifested as decreases in plants biomass above and below ground (roots, leaves and shoot), which can further result in a reduction of carbon inputs into the soil (Pulido-Moncada et al. 2022; Soares et al. 2015).

Considering these processes, soil compaction has a strong impact on water and nutrient cycling and some of the major risks that have been associated with compaction include: (1) crop yield decline, (2) losses of soil organic carbon and (3) nitrogen losses through increased nitrous oxide emissions and nitrate leaching. Despite acknowledging these risks, understanding how different processes interact and quantifying the long-term effects on soil functions and the environmental and economic consequences of soil compaction remain challenging. This is associated with (I) a lack of solid data on the spatial and temporal extent of soil compaction (Håkansson and Lipiec 2000), (II) the resource limitations for measuring and quantifying long-term impacts of soil compaction in a systematic way and, (III) the complexity in understanding how the different compaction-impacted soil processes interact and what the relative importance of the compaction level, soil texture, crop and climate are. Mechanistic modelling of soil compaction and its impacts on soil physical properties may be combined with existing agroecosystem models for deriving new insights to understand the long-term impacts of compaction on soil (dis)services (Chamen et al. 2015) in a systematic way.

In this work, we aimed at systematically assessing the long-term impact of soil compaction on crop yield, soil organic carbon stocks, nitrous oxide emissions and nitrate leaching. For this, we established the following objectives:

1. To compile and report literature evidence on key aspects and trends of how compaction impacts crop yield, soil organic carbon stocks, nitrous oxide emissions and nitrate leaching.
2. To establish a modelling framework for systematic incorporation of soil compaction-induced changes in soil structure into an agroecosystem modelling approach.
3. To establish and conduct simulations in a base-case modelling scenario (and other scenarios with slight variations of textures, climatic conditions and recovery rates) representing common pedoclimatic conditions of European croplands.
4. To dissect modelling results to assess how modelled soil (dis)services capture salient features of literature data and to discuss the underlying physical processes leading to such results.

2 | Evidence of Soil Compaction Effects on Crop Yield, Soil Organic Carbon Stocks and Nitrogen Losses from Soil: A Data Compilation

We compiled empirical data from the literature to identify trends in the effects of soil compaction on crop yield, soil organic carbon stocks, nitrous oxide emissions and nitrate leaching and use these data for comparisons with modelling results. The criteria for the literature search was to obtain studies that: (i) compared compacted and non-compacted (control) soils, (ii) were conducted in field conditions (iii) in cropland or grassland (but not in forests). For crop yield, we selected the studies from the database reported in the meta-analysis by Obour and Ugarte (2021). For soil organic carbon stocks, we conducted a search in WebofScience for publications that simultaneously contained a term alluding to compaction ('soil compaction', 'compaction', 'wheeling', 'treading' and 'trampling') and a term alluding to soil organic carbon stocks ('carbon,' 'soil organic carbon', 'soil carbon', 'carbon stocks'). Similarly, for nitrous oxide emissions, we selected the studies from the database reported in the meta-analysis by Hernandez-Ramirez et al. (2021). For nitrate leaching, we conducted a search in WebofScience for publications that simultaneously contained a term alluding to compaction ('soil compaction', 'compaction', 'wheeling', 'treading' and 'trampling') and a term alluding to nitrate leaching ('nitrate', 'nitrate leaching', 'NO_3 leaching', 'NO3'). All the selected studies ($n = 60$) measured at least one of the variables of interest for one (or various) compaction treatment(s) and a non-compacted control treatment.

Our literature search comprises 23, 8, 22 and 7 studies for crop yield, soil organic carbon stocks, nitrous oxide emissions and nitrate leaching, respectively. From these studies, we used 183, 10, 110 and 29 paired comparisons (compacted vs. non-compacted) for crop yield, soil organic carbon stocks, nitrous oxide emissions and nitrate leaching, respectively. The effect of soil compaction on crop yield and nutrient dynamics can be observed immediately after compaction, which facilitates experimental planning and is reflected in a larger number of studies for these variables. In contrast, effects on soil carbon stocks may take several decades to build up and hence studies targeting soil compaction effects on soil carbon stocks are limited. Most studies correspond to temperate regions and loamy soils (Tables S1–S4). We extracted

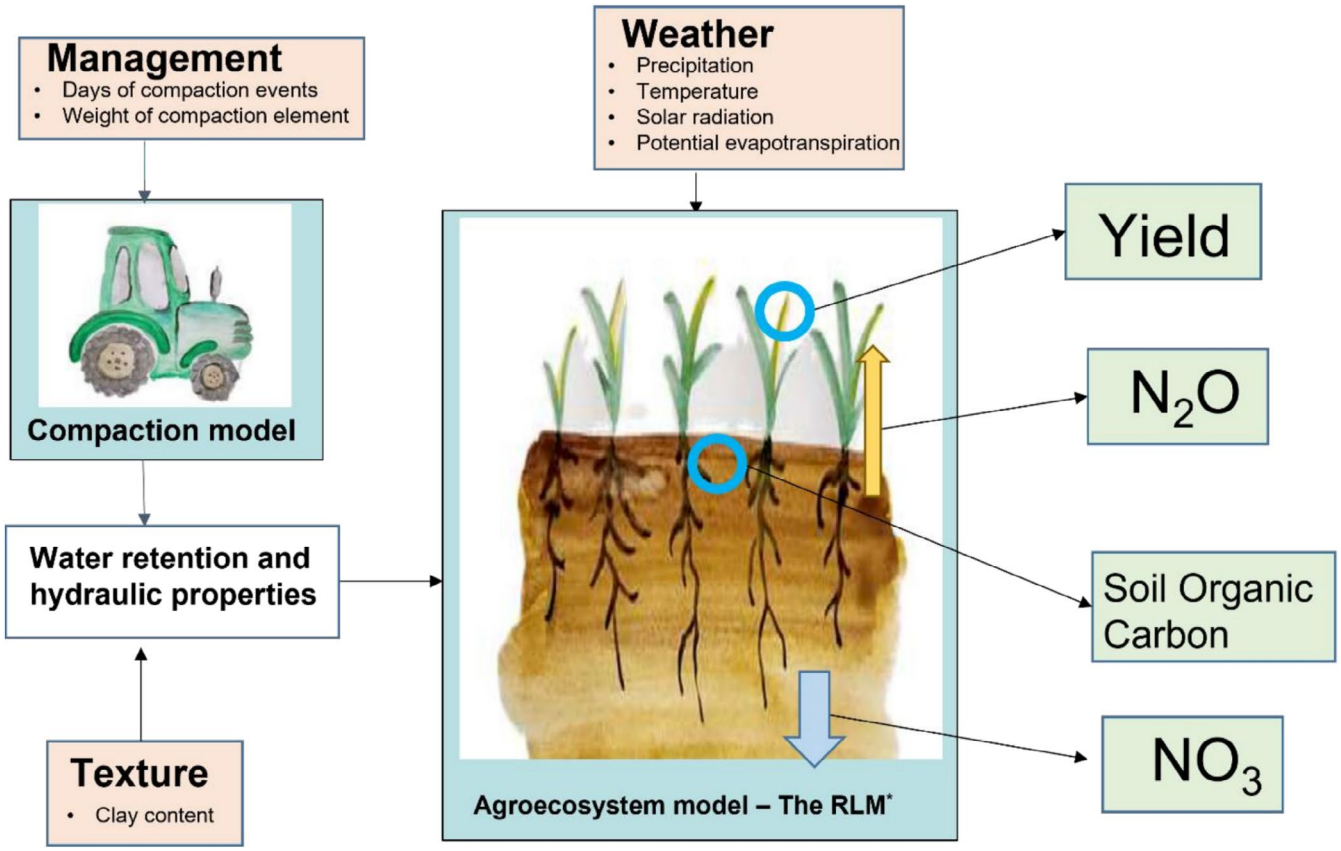

FIGURE 1 | Schematic representation on the modelling approach used in this study: The RLM-SCC model. A soil compaction model is used to systematically simulate changes in soil structure induced by a compaction event. The modelled changes in soil structure are then infused in an agro-ecosystem model. By doing this, the modelling framework enables simulation of compaction-induced changes in soil state variable and their impacts on soil processes and functions. Model inputs and outputs are presented in orange and green blocks, respectively. The Rothamsted Landscape Model (RLM Coleman et al. 2017) was used in this study to simulate crop growth and C- and N-cycling. Illustrations by Dr. Alice Johannes (Agroscope, Switzerland).

absolute and relative (i.e., compacted/control) values of each variable, time since compaction and clay content (Tables S1–S4), as these metrics allow comparing impacts of compaction across heterogeneous studies. When the clay content was not available but the textural class was reported, we used the mean clay content for such class based on Carsel and Parrish (1988) to situate them in the correct range of clay contents.

3 | Soil Structure-Based Modeling Framework to Account for Compaction in Agroecosystems: The RLM-SCC Model

We expanded the modelling framework presented in Romero-Ruiz et al. (2024) used to evaluate grazing-induced compaction to simulate vehicle traffic compaction effects on soil processes related to crop growth, C- and N-cycling. The framework integrates (i) a soil compaction model (Romero-Ruiz, Monaghan, et al. 2023) and (ii) an agroecosystem model (the Rothamsted Landscape Model, RLM; Coleman et al. 2017). Soil compaction-induced changes in soil physical properties (macroporosity, bulk density and K_{sat}) are calculated by the soil compaction model at daily time steps, depending on whether there is compaction or recovery occurring on a given day and these are updated in the RLM. This framework, termed here as the 'RLM-SCC' model (Rothamsted Landscape Model-Soil CompaCtion module), allows for systematically quantifying impacts of compaction on soil states and (dis)services (Figure 1).

By changing the bulk density, macroporosity and saturated hydraulic conductivity, the integration of the compaction model (developed first by Romero-Ruiz, Monaghan, et al. 2023) into the RLM (Coleman et al. 2017), allows to model changes in the variables of interest: crop yield, soil carbon, nitrous oxide emissions and nitrate leaching. More specifically, the RLM-SCC model induces changes in hydraulic and mechanical properties of simulated soils. In terms of hydraulic properties, changes in the saturated hydraulic conductivity reflect in (i) changes in soil water dynamics controlling water availability for root water uptake in the crop model (Section 3.3), (ii) changes in the water filled pore space that is used (in addition to total porosity also modified by compaction) to calculate nitrous oxide emissions by nitrification and denitrification (Section 3.3), (iii) changes in the relative permeability of soils (Section 3.3) ultimately determining daily water flow relevant for nitrate leaching (Section 3.4) and (iv) changes in daily carbon decomposition rates (Section 3.4). The changes in bulk density are used to calculate the soil penetration resistance that controls the growth rate of roots, impacting: (i) root water

and nutrient uptake in the crop model (Section 3.3) and (ii) ultimately impacting water dynamics, which affects all variables as described above. The details of the modelling framework are presented in the following sections.

3.1 | Soil Compaction Model

Integrating modelled impacts of compaction in an agroecosystem model, which typically have a simplified representation of soil structure, requires a matching simplified description of soil compaction impacts on soil structure. The soil compaction model by Romero-Ruiz, Monaghan, et al. (2023) was developed for this purpose. In this work, this model was used to systematically calculate the temporal dynamics (i.e., compaction events and recovery at different rates) of three key soil properties impacted by compaction: soil bulk density (ρ), macroporosity (w_{mac}) and saturated hydraulic conductivity (K_{sat}). A compaction event produces an irreversible strain, ϵ_v, which is modelled using information about the initial (i.e., prior to compaction) strain ϵ_0, the normal load and duration of stress application and the soil rheological properties as (Ghezzehei and Or 2001):

$$\epsilon_v(t) = \left[\epsilon_B^2 S_{sm}(t)^{N_v}(1-\cos(\omega t)) + \epsilon_0^2\right]^{\frac{1}{2}}, \quad (1)$$

where t is the time, ω is the loading frequency (i.e., related to vehicle speed), ϵ_B comprises information of the soil rheological properties and the characteristics of the compaction event (e.g., proportional to the square of the stress induced by a vehicle), $S_{sm} = \theta_{sm}/\phi_{sm}$ is the degree of water saturation in the soil matrix, where θ_{sm} is the water content in the soil matrix and ϕ_{sm} *is* the total porosity of the soil matrix and N_v is an empirical exponent accounting for the soil compaction sensitivity to soil water content changes. Note that in this modelling framework, S_{sm} is calculated by the RLM and transferred to the compaction model on days of simulated compaction events (e.g., trafficking days).

The compaction induced strain is then used to consecutively calculate ρ, the total porosity (ϕ_T), w_{mac} and K_{sat}. The ϕ_T is calculated from ρ and the particle density (assumed to be 2.65 g cm^{-3}), the w_{mac} is calculated from the change in ϕ_T assuming the net change in total porosity equals the net change in macroporosity and K_{sat} is calculated as a function of the macroporosity based on the dual-porosity model by Durner (1994). The model is strongly sensitive to ϵ_B and N_v as shown and discussed by Romero-Ruiz, Monaghan, et al. (2023) using an example of parameter estimation using a Markov Chain Monte Carlo approach.

The soil compaction model computes recovery of soil properties as a function of time following a compaction event. The shape of the soil structure recovery function is unknown and will depend on pedoclimatic conditions. As a first approach, here we simulate recovery of the compaction-induced strain based on the model by Meurer et al. (2020), with an empirical exponential function given by:

$$\epsilon_v(d_r) = \epsilon_0 - (\epsilon_0 - \epsilon_i)e^{-d_r/\lambda_{tr}}, \quad (2)$$

where ϵ_i is the soil strain, representing the strain resulting after the compaction event, d_r is the number of days after the compaction event and λ_{tr} [days] is the recovery rate.

3.2 | The Agroecosystem Model

The Rothamsted Landscape Model (RLM) discretizes the soil into three layers with model-defined interfaces at 0.23 and 0.46 m (final layer ends at 1 m). They represent a topsoil, an upper subsoil layer and a lower subsoil layer. This choice was made by Coleman et al. (2017) to balance vertical heterogeneity of the soil profile and computation times, which are important when coupling models with optimisation algorithms and under spatially variable and long-term climate projections. In the following, we describe how water flow, nitrogen dynamics, crop growth and carbon cycling are modelled and affected by compaction in RLM-SCC.

3.2.1 | Soil Water and Temperature Dynamics

RLM uses a bucket-type modelling approach to simulate water flow in the soil profile. Water retention and hydraulic properties are modelled using the dual domain approach (Durner 1994) as:

$$S_e = \frac{\theta-\theta_r}{\phi_T-\theta_r} = w_{sm}\left[1+(\alpha_{sm}h)^{n_{sm}}\right]^{1-\frac{1}{n_{sm}}} + w_{mac}\left[1+(\alpha_{mac}h)^{n_{mac}}\right]^{1-\frac{1}{n_{mac}}}, \quad (3)$$

and

$$K_{soil} = r_k K_{sm}\frac{\left(w_{sm}S_{e_{sm}} + w_{mac}S_{e_{mac}}\right)^{0.5}}{\left(w_{sm}\alpha_{sm} + w_{mac}\alpha_{mac}\right)^2} \left(w_{sm}\alpha_{sm}\left[1-\left(1-S_{e_{sm}}^{\frac{n_{sm}}{n_{sm}-1}}\right)^{1-\frac{1}{n_{sm}}}\right] + w_{mac}\alpha_{mac}\left[1-\left(1-S_{e_{mac}}^{\frac{n_{mac}}{n_{mac}-1}}\right)^{1-\frac{1}{n_{mac}}}\right]\right)^2, \quad (4)$$

where h is the pressure head, S_e is the effective saturation of the soil, θ_r is the residual water content, n_i is the van Genuchten (1980) exponent (related to soil texture) and α_i is related to the inverse of the air-entry pressure. In Equation (4), K_{soil} is the pressure head (i.e., water content) dependent soil hydraulic conductivity (also known as relative permeability). The saturated hydraulic conductivity of the soil, $K_{sat} = r_k K_{sm}$, is defined as the product of the saturated hydraulic conductivity of the soil matrix, K_{sm} and the ratio $r_k = K_{sat}/K_{sm}$ that is a function of soil macroporosity. The initial macroporosity and K_{sat} are input variables of the model, then updated by the compaction model in response to compaction events as detailed by Romero-Ruiz, Monaghan, et al. (2023).

The soil temperature in each model layer is modeled as a function of the daily air temperature and the depth of each model layer. The soil temperature is then calculated using a depth dependent exponential log function as typically done in agroecosystem models (Bieger et al. 2017).

3.2.2 | Crop Growth

The crop module uses a light use efficiency (LUE, g dry matter MJ^{-1}) based approach to calculate biomass production (Monteith 1977). The rate of biomass (B_{crop}) produced each day is given by:

$$\frac{dB_{crop}}{dt} = Q\phi W_{rf} N_{NI} P_{NI}, \tag{5}$$

where Q is the intercepted photosynthetically active radiation (PAR, MJ PAR m^{-2} surface area), which depends on the solar radiation and canopy leaf area, ϕ is the crop specific light use efficiency (LUE), W_{rf} is a transpiration reduction factor and N_{NI} and P_{NI} are nitrogen and phosphorus nutrition indices varying between 0 to 1 for residual and optimal nutrient contents calculated from nutrient demand (Shibu et al. 2010). The biomass formed is partitioned between roots, stem, leaves and storage organs, based on the development stage (Boons-Prins et al. 1993; Wolf 2012). The root system is initialized at the emergence stage from the top of the soil profile, at which point roots grow at a daily rate until a maximum crop specific rooting depth. The rooting depth is then updated adding a growth rate that is calculated from the root biomass availability coefficient (see figure 2 in Shibu et al. 2010) and scaled as a function of the soil penetration resistance (SR) (Azam et al. 2014; Gao et al. 2016). The SR is affected by bulk density and hence by the compaction model. The root density distribution is modelled using an exponential function with maximum at the soil surface and decaying to zero at the daily rooting depth (Gerwitz and Page 1974). The RLM then calculates a layer-specific root density by integrating the daily root density function (which is a continuous function) within each layer domain. The roots take nitrogen from the soil layers based on demand (considering all organs) and nitrogen availability in the soil and nitrogen is then distributed proportionally to all plant organs (Coleman et al. 2017; Shibu et al. 2010). Convection and diffusion of nutrients through the plants' organs are not explicitly considered.

The transpiration reduction factor (W_{rf}) is defined as the ratio of actual transpiration (mm day^{-1}) to potential transpiration (mm day^{-1}) and is summed for all layers across the soil profile as:

$$W_{rf} = \sum \frac{A_{T\,i}}{P_{T\,i}}, \tag{6}$$

where P_T is the daily potential transpiration. Note that W_{rf} is indirectly affected by compaction through the compaction impacts on soil water dynamics.

The amount of the actual transpiration stemming from layer i is given by:

$$A_{Ti} = \frac{P_{Ti} W_{Si}^2 F_{RLi}}{\sum W_{Si} F_{RLi}}, \tag{7}$$

Here, F_{RL} is the fraction (related to the total root biomass) of root in each soil layer and W_S describes the impact of water content on the water stress function (Li et al. 2001). This impact of water content is based on the method described in Feddes (1978) given by:

$$W_s = \begin{cases} \dfrac{\theta_s - \theta}{\theta_s - \theta_a}, & \text{for } \theta > \theta_a \\ 1, & \text{for } \theta_a > \theta > \theta_a \\ \dfrac{\theta - \theta_w}{\theta_d - \theta_w}, & \text{for } \theta_d > \theta > \theta_w \end{cases} \tag{8}$$

where θ_a is the water content at −5 kPa, θ_d is the water content at −40 kPa and θ_w is the water content at the permanent wilting point (i.e., a soil matric potential of −1500 kPa).

3.2.3 | Nitrogen Cycle

In RLM, soil mineral N consists of N in ammonium (NH_4^+) and nitrate (NO_3^-). The concentration of NO_3- in layer i, ($\gamma_i NO_3$) is given by:

$$\gamma_i NO_3(l) = \frac{N_{NO3}(i)}{\theta_i}, \tag{9}$$

where $N_{NO3}(i)$ is the NO_3- (kg N ha^{-1}) in layer i, $i = 1$, 2 and 3 and θ_i is the water content of layer i. The amount of NO_3- (kg N day^{-1}) that moves down each layer i is given by:

$$F_{NO_3} = max\left(0 \;\; min\left\{N_{NO_3}(i-1)_{\gamma i NO_3}(i-1)F_W(i)\right\}\right), \tag{10}$$

where $F_W(i)$ is the amount of water that flows from layer i to layer $i+1$. The nitrate that moves down from layer 3, $F_{NO3}(3)$, is N leached out of the profile.

The rate of nitrification depends on water filled pore space (θ/θ_s), soil temperature (T), soil moisture (θ) and soil pH (S_{pH}). In the model, the amount of N_2O (kg N ha^{-1} day^{-1}) produced from a given amount of NH_4+ ($N_{NH4}(i)$) in layer i is given by:

$$N_{N2O} = \kappa_{N2O} N_{NH4}(i) S_{pH}(i)\left(1 - \frac{\theta_i}{\theta_s(i)}\right), \tag{11}$$

where κ_{N2O} is a constant that takes the value of 0.0001 (Coleman et al. 2017). The amount of nitrate (kg N ha^{-1} day^{-1}) produced from soil NH_4+ is given by:

$$N_{NO3}(\mathrm{i}) = max\left[\left(N_{NH4}(i) - N_{N2O}(i) - N_{min}\right)\left(1 - e^{-k}\right) f\left(T_i\right) g\left(\theta_i\right) \;\; 0\right], \tag{12}$$

where N_{min} is the minimum amount of NH_4+ that must be in the soil for nitrification to occur (we assumed $N_{min} = 0.05$; Coleman et al. 2017), k is a constant for nitrification that is set at 0.15 in this study (as in Coleman et al. 2017) and $f(T_i)$ and $g(\theta_i)$ are functions that describe the effect respectively of temperature and moisture on nitrification (Godwin and Allan Jones 1991).

Denitrification is an anaerobic process whereby the NO_3- in the soil is reduced to nitrous oxide and nitrogen gas (N_2). N_2O emissions (kg N ha^{-1} day^{-1}) from denitrification are modelled as:

$$N_2O(i) = 0.000735 N_{NO3} f\left(\theta/\theta_S(i)\right) \exp\left[-0.00045\left(T_i - 23.65\right)^2\right], \tag{13}$$

where $\theta/\theta_S(i)$ is the water filled pore space in each layer i (Parton et al. 1996):

$$f\left(\theta/\theta_S(i)\right)=\left(\frac{\theta/\theta_S(i)-b}{a-b}\right)^{d\left(\frac{b-a}{a-c}\right)}\left(\frac{\theta/\theta_S(i)-c}{a-c}\right)^{d}, \quad (14)$$

The nitrogen taken up by the crop each day is taken from the nitrate pool with an upper limit of 6 kg N ha^{-1} day^{-1} (Semenov et al. 2007). The empirical factors in Equation (13) were calculated to fit data from various experiments in the UK as described by Coleman et al. (2017). Note that in this implementation, dynamics effects of soil pH (assumed constant) as well as competing oxygen demands for nutrient and carbon cycling are not considered.

3.2.4 | Carbon Cycle

The soil total organic carbon (TOC) model in RLM is based on the Rothamsted carbon model, RothC (Coleman and Jenkinson 1996). Soil total organic carbon is split into four active compartments and a small amount of inert organic matter (IOM). The four active compartments are decomposable plant material (DPM), resistant plant material (RPM), microbial biomass (BIO) and humified organic matter (HUM). Each compartment decomposes by a first-order process with its own rate constant. The IOM compartment is resistant to decomposition. Decomposition of each of the four active pools is modified by rate modifying factors for temperature, moisture and plant retainment. An active compartment containing X Mg C ha^{-1} declines to $X\,e^{-a_c b_c c_c d_c t}$ Mg C ha^{-1} after a given time t, where a_c, b_c, c_c and d_c are the rate modifying factors for temperature, moisture, soil cover and compartment, respectively and t is the time. The temperature modifying factor is given as:

$$a_c=\frac{47.91}{1+e^{\frac{106.06}{T+18.27}}}, \quad (15)$$

where T is the average daily temperature (°C). The moisture modifying factor is given by:

$$b_c=1 \qquad for\ S_{acc}<0.44S_{max}$$
$$b_c=0.2+(1-0.2)\frac{S_{max}-S_{acc}}{S_{max}-0.44S_{max}} \qquad otherwise \quad (16)$$

where S_{max} and S_{acc} are the maximum and accumulated soil moisture deficit, respectively. S_{acc} is defined by month (a full description of the carbon model can be found in Coleman and Jenkinson 2014) and S_{max} is defined as a function of soil texture as:

$$S_{max}=-\left(20.0+1.3(\%clay)-0.01(\%clay)^2\right). \quad (17)$$

3.3 | Calibration of the Soil Compaction Model

To calibrate the soil compaction model, data on soil stress, changes in bulk density, macroporosity and K_{sat} are needed. However, such datasets are scarce. Here, we calibrated the soil compaction model using data from a compaction event on a loam soil, the most dominant soil texture globally (Michli et al. 2006), conducted in Zürich, Switzerland (Keller et al. 2017).

The pre-compaction bulk densities were used as initial information and we performed a grid search to infer the strains ε_v that reproduce post-compaction soil bulk densities and an estimation of the corresponding mean normal stress as a function of depth (see Figure S1 in the Supporting Information, SI). For validation, the soil compaction model was then used to predict pre- and post-compaction macroporosities (Figure S1c) and saturated hydraulic conductivities (Figure S1d), for which normalized root mean square errors of 0.23 (for macroporosity) and 8.13 (for the logarithm of the saturated hydraulic conductivity) were obtained, considering an error of 5% in each case. The inferred strain was $\varepsilon_{vbase}=0.0355$. The underscript *base* is used to indicate that this inferred variable refers to the base case for simulations, as described later. Since ε_v is proportional to the induced stress by a vehicle (Ghezzehei and Or 2001), different levels of compaction are obtained by multiplying the inferred ε_{vbase} by a given factor. This factor is termed here as normalized wheel load, δ_c.

By predicting changes in bulk density, macroporosity and K_{sat} as a function of their pre-compaction values and wheel load, this model calibration allows creating different realistic compaction levels used in the simulations within RLM-SCC, as described in the following section.

3.4 | Model Simulations Scenarios: Compaction Levels, Soil Textures, Weather Data and Soil Structure Recovery Rates

We established a series of modelling scenarios (Table S5) to quantify the impact on different levels of compaction on crop yield, soil organic carbon stocks, nitrous oxide emissions and nitrate leaching and to quantify how they are influenced by soil texture, climate and soil structure recovery rates. For this, we first established a base-case modelling scenario using representative soil and weather conditions from the continental Europe pedoclimatic zone. We then varied clay content, mean annual precipitation, mean annual temperature and soil structure recovery rates. These variations (i.e., scenarios) were tested independently to assess the isolated impacts of these factors. For simplicity, all other agroecosystem model parameters remained the same in all modelled scenarios (see default values in Coleman et al. 2017). In general, the parameter ε_{vbase} and the water content at the moment of compaction depend on soil texture and climate. Yet, in this work the compaction levels were created considering ε_{vbase} to be the same in all modelled scenarios and a fixed water content at field capacity. This was intentionally prescribed to enable investigating the effects of soil compaction across different scenarios for the same compaction level.

The scenario-simulation approach used a base scenario designed to represent typical conditions of compacted agricultural systems, hypothesizing that such a case scenario should reproduce salient features of trends observed in the literature. This allows us to situate the modelling results in the context of heterogeneous observations reported in the literature (Section 2), where site-specific pedoclimatic and experimental conditions differ yet are expected to share similar compaction-induced modifications of underlying processes. The base case scenario was then modified with variations in soil texture, climate and recovery rate to explore how these factors influence the modelling outputs in an independent way, which was

expected to expand the ranges of conditions and better cover literature data. We do not consider different recovery rates for different soil layers, repeated wheeling, fertilisation and other management strategies to avoid introducing further elements difficulting interpretation. This allows us to provide an overview of compaction impacts on the investigated variables for a range of plausible pedoclimatic conditions and can serve as a basis for future studies. To compare with literature observations (Section 2), we simulated crop yield, soil organic carbon stocks of the topsoil (to be in agreement with all literature data), annual nitrous oxide emissions and annual nitrate leaching.

3.4.1 | Base Case Scenario

For the base case simulation scenario, the model was run using a 50 year-long weather prediction from climate projections for a European continental pedoclimatic zone by ACCESS-CM2 (Bi et al. 2020). These data correspond to a mean annual precipitation of 800 mm and a mean annual temperature of 8.5°C (Figure S2). The soil was considered to have a clay content of 25%. We considered a one-time soil compaction event that was modelled considering one vehicle passage (two axles). The RLM model was previously initialized by running a 100 years simulation using weather data from the first year of the projected data (Coleman et al. 2017). Recovery of soil properties was not considered in the base case scenario and hence the model was run with compacted inferred properties for all the simulated years. In the base case scenario, we considered 30 levels of compaction obtained by varying the normalized wheel load from 0.05 to 1.5 with 0.05 increments (corresponding to wheel loads from 0.4 Mg to 12 Mg, with increments of 0.4 Mg). Therefore, the base case scenario comprises 30 simulations for 30 different levels of compaction, each with a corresponding set of modelled bulk densities, macroporosities and saturated hydraulic conductivities. For simplicity, all the simulations presented in this study were done for one crop only: winter wheat, the most important crop in Europe (harvested area approximately 62.7 Mha, https://data.europa.eu/doi/10.2762/722428). Sowing and harvesting dates were 1st of October and 15th of July (Heller et al. 2024), respectively (Figure S2). Inputs of N through atmospheric deposition were set to 18 kg N $year^{-1}$ (Goulding et al. 1998) and distributed evenly throughout the year as nitrate. For simplicity and to avoid confounding impacts of fertilisation, no fertilizer application was considered in our simulations.

3.4.2 | Soil Texture Scenarios

To investigate the role of soil texture, we considered three clay contents: 15%, 25% (base case, see Section 3.4.1) and 35%, covering the range of clay contents found in the considered literature studies (Tables S1–S4). The impacts of soil texture were incorporated by considering clay-content dependent water retention properties based on the data compilation presented (Carsel and Parrish 1988). The van Genuchten model parameters were obtained by linear regression for θ_r, θ_s, $log(\alpha)$ and $log(k_s)$ as a function of clay content and by fitting an exponential function between n and clay content (Figure S3). Note that k_s here refers to the saturated hydraulic conductivity of the soil matrix, which differs from K_{sat} that is the saturated hydraulic conductivity of the dual-domain soil (considering the soil matrix and macropores) as explained in Section 3.2. The texture simulations scenarios were done using the same weather data and considering the 30 levels of compaction as the base case scenario (see also Table S5).

3.4.3 | Changes in Mean Annual Precipitation: Precipitation-Scenarios

Disentangling effects of soil compaction in different climates is challenging as precipitation and temperature typically vary simultaneously. We opted for running model simulations varying the precipitation and temperature independently, to isolate the respective effects. We considered two scenarios with lower or higher mean annual precipitation compared with the base case scenario, namely 400 and 1200 mm per year, which were obtained by multiplying daily precipitation from base case scenario by 0.5 and 1.5, respectively. The rest of the weather variables (e.g., solar radiation) were kept the same. The precipitation scenarios were made using the soil with 25% clay content and with the same 30 compaction scenarios considered as in the base case (Table S1).

3.4.4 | Changes in Mean Annual Temperature: Temperature-Scenarios

Similar to the previous section, we ran model simulations varying the mean annual temperature independently of changing other driving variables. In the base case, the mean annual temperature was approximately 8.5°C and the minimum, mean and maximum monthly temperature of the growing season (October–July) were approximately −3°C, 4°C and 16°C, respectively. We considered two additional scenarios, one with a mean annual temperature of 6°C and one with a higher mean annual temperature of 11°C. These were obtained by subtracting and adding, respectively, 2.5°C to all the daily temperatures of the base case. All other weather variables were kept the same. The temperature scenarios were made using the soil with 25% clay content and with the same compaction scenarios considered as in the base case (Table S5).

3.4.5 | Changes in Soil Structure Recovery Rates: Recovery-Scenarios

We considered four soil structure recovery scenarios: (1) no recovery (base case, corresponding to $\lambda_{tr} = inf$ in Equation 2), (2) full recovery after 5 years (corresponding to a recovery rate of $\lambda_{tr} = 1.6$ in Equation 2), (3) full recovery after 10 years (corresponding to a recovery rate $\lambda_{tr} = 2.3$ in Equation 2); (Berisso et al. 2012) and (4) full recovery after 20 years (corresponding to a recovery rate $\lambda_{tr} = 4.3$ in Equation 2). The scenarios represent realistic scenarios of soil compaction recovery, which could take several years to decades (Berisso et al. 2012; Blackwell et al. 1985; Peng and Horn 2008). In the modelled recovery-scenarios, soil structure recovery strictly refers to the recovery of bulk density, macroporosity and saturated hydraulic conductivity. Note

that, in the recovery scenarios, the model runs with dynamics changes in soil properties affecting processes described in Section 3.2 and no additional assumptions were made on how recovery impacts the model outputs. For simplicity, these structural properties and all depths were considered to recover at the same recovery rate λ_{tr} ensuring full recovery of physical properties at the same time. Time for "full recovery" after compaction was defined as time needed until the relative difference between pre- and post-compaction bulk density was lower than 1%. No re-compaction events (i.e., repeated wheeling events) were considered in any scenarios.

4 | Results

4.1 | Literature Data Synthesis

The combination of the elements: (i) compaction-induced damage, (ii) soil texture and (iii) climate is in general different across studies, which increases the variability of the reported data and results in a lack of clear trends for all variables. Yet, the number of studies was limited, which made it unfeasible to divide them into groups according to soil textures, climate and compaction level. Given these limitations reflecting a gap in literature evidence, we opted to present average trends across all gathered studies for a given variable despite representing different compaction levels, soil textures, climates, length of experiments, etc. To report the data in a meaningful way, we plotted the variables of interest from all selected studies in relative terms (i.e., compacted/non-compacted) and as a function of time after the experimental compaction event (Figure 2).

About 85% of the studies reported relative crop yields lower than 1, ranging from 0.2 to 1.2 with an average value of 0.82 (Figure 2a). Compaction did not have a consistent effect on soil organic carbon stocks and the relative values for SOC stocks ranged from 0.5 to 1.4 with an average value of 1.1 (Figure 2b). The relative nitrous oxide emissions were typically higher than 1, ranging from 0.4 to 29 with an average of 3.2 (median of 1.6), indicating a threefold increase on average in N_2O emissions due to compaction (Figure 2c). Increases in N_2O emissions did not seem to follow a trend as a function of time since compaction (Figure 2c). Data for nitrogen leaching were typically reported for 1-year-long periods after compaction only. They ranged from 0.4 to 1.7 (average value of 1.02) and did not present any clear temporal trend (Figure 2d).

4.2 | Modelling Results

4.2.1 | General Trends in the Base Case Simulations

The modelled compaction-induced changes in crop yields, soil carbon stocks, nitrous oxide emissions and nitrate leaching under the base case scenario agreed with the ranges observed in the literature (Figure 3). The yearly relative change in yield fluctuated around a mean value of 0.77 (literature data average was 0.82). An average decrease in soil organic carbon stocks due to compaction of about 4.3% (literature data average was a 10% increase) after 50 years was predicted by the model (Figure 3b). The model predicted an average 2.5-fold relative increase (literature data average was 3.2) in annual cumulative nitrous oxide emissions, which remained at similar levels during the full simulation (Figure 3c). The average cumulative annual nitrate leaching increased by 15% due to compaction (literature data average was a 2% increase) in the base case scenario (Figure 3d).

4.2.2 | Compaction Impacts for Different Soil Textures

Crop yields were predicted to decrease with compaction for most years across all clay contents, with the relative yield values fluctuating around 0.65, 0.77 and 0.88 for 15%, 25% and 35% clay content, respectively (Figures 3 and 4). The modelled ranges (related to the 30 different compaction levels) of relative yields were similar for all clay contents (Figure 3a). Soil organic carbon stocks generally decreased due to compaction for all soil textures, with some small increases at certain times (Figure 3b). Relative carbon stocks changes were similar for all three clay contents, corresponding to losses of 4.6%, 4.3% and 3% for 15%, 25% and 35% clay content, respectively (Figure 3b). The relative nitrous oxide emissions increased for all clay contents (Figure 3c). The relative increase in nitrous oxide emissions was highest for the lowest clay content, with average increases of 4, 2.5 and 1.7 times for 15%, 25% and 35% clay content, respectively (Figure 3c). The model predicted a 22% increase in nitrate leaching for soil with 15% clay content, a 15% increase for 25% clay content and a decrease of 10% for 35% clay content (Figure 3d).

4.2.3 | Compaction Impacts for Different Precipitation-Scenarios

Crop yield decreased with compaction for all precipitation regimes (Figures 5 and 6). The effects of soil compaction in crop yield were predicted to be the lowest in the low precipitation scenario, with relative values fluctuating around 0.89, 0.77 and 0.73 for 400, 800 and 1200 mm $year^{-1}$. This is consistent with increasing compaction-induced losses of nitrate with increasing precipitation (Figure 5d). Fluctuations of crop yield were larger for lower mean annual precipitation (Figures 5a and 6a) Soil organic carbon stocks decreased by 3.4%, 4.3% and 3.7% for 400, 800 and 1200 mm $year^{-1}$, respectively (Figure 5b). The relative carbon stocks had similar ranges for all precipitation scenarios (Figure 7b). Nitrous oxide emissions increased in all precipitation regimes, with average relative emissions of 2.5, 2.5 and 2.3 for 400, 800 and 1200 mm $year^{-1}$, respectively (Figure 5c). The ranges in relative yearly nitrous oxide emissions were similar for all precipitation regimes (Figures 5c and 6c). The cumulative nitrate leaching increased with soil compaction for the precipitation regimes of 800 and 1200 mm $year^{-1}$ (with increases of 14% and 4%, respectively), but was unaffected by compaction for the 400 mm $year^{-1}$ regime (Figure 5d).

4.2.4 | Compaction Impacts for Different Temperature-Scenarios

Crop yield was predicted to decrease with compaction for the 6°C and 8.5°C scenarios, while it was less affected by compaction in the 11°C regime (Figures 7a and 8a). The average relative yields were 0.71, 0.77 and 1 for 6°C, 8.5°C and 11°C,

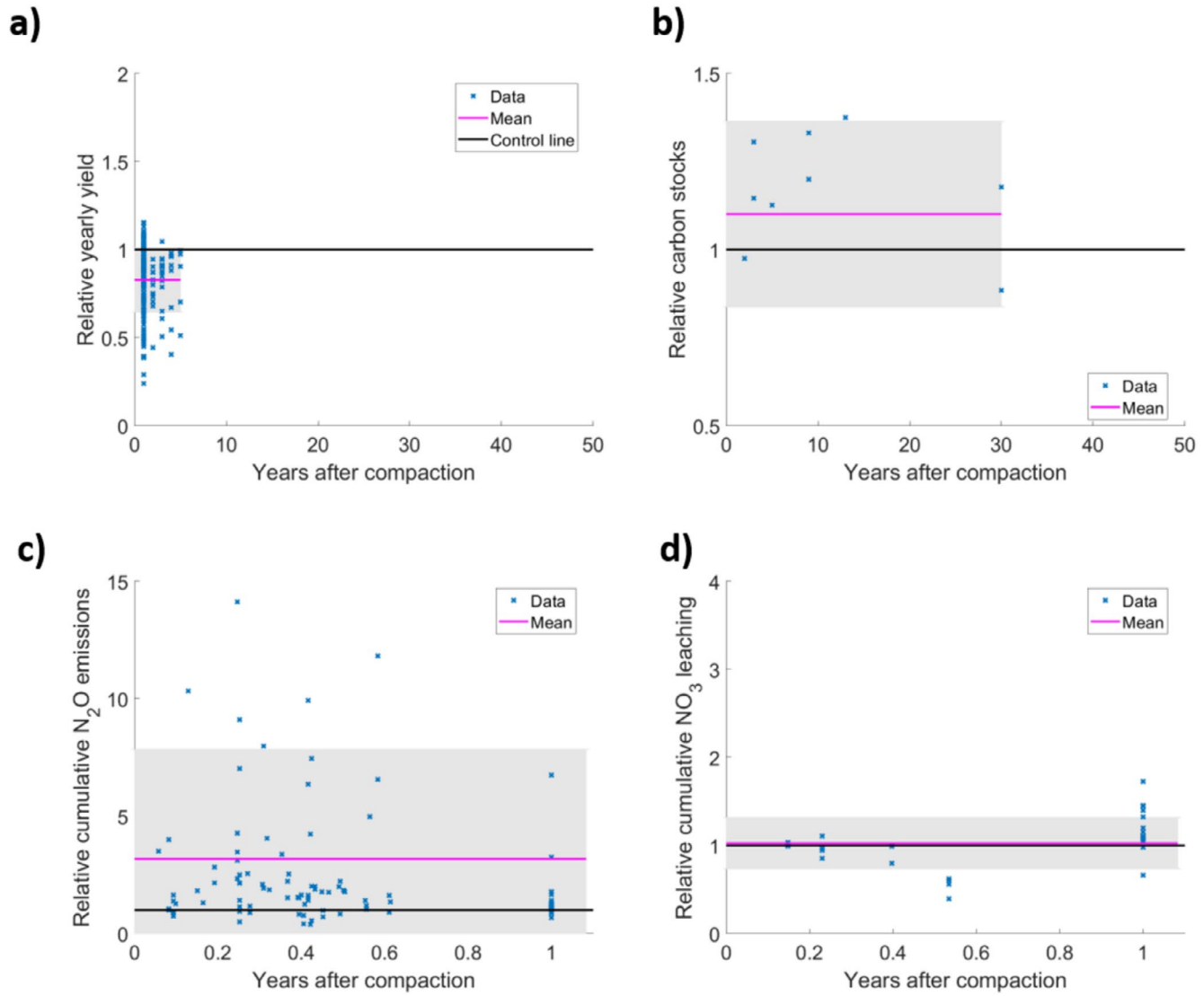

FIGURE 2 | Literature data comparing impacts of soil compaction on crop yield (a), soil organic carbon stocks (b), nitrous oxide emissions (c) and nitrate leaching (d). The figure reports relative changes (i.e., the ratio of compacted to non-compacted), the control line (compaction/no compaction = 1; black line), the mean value of the data (magenta line) and the range (grey, standard deviation of the mean of the relative values). Note the different scales on the *x*-axes, which are in years after compaction for crop yield and soil organic carbon stocks and in months after compaction for nitrous oxide emissions and nitrate leaching. Note that the horizontal axis in (a) and (b) goes from 0 to 50 years after compaction despite the lack of data under this extended range. This was done to be consistent with figures corresponding with simulations that do cover this range.

respectively (Figure 7a). This is consistent with increasing compaction-induced losses of nitrate with decreasing temperature (Figures 5d and S8d). Note that despite having an average rate of 1, yield decreased for the first 20 years for the 11°C scenario. Hence, the model predicted similar trends in relative carbon stocks for all temperature regimes, decreasing by 2.8%, 4.3% and 4.6% for 6°C, 8.5°C and 11°C, respectively (Figure 7b). An increase in nitrous oxide emissions due to compaction was simulated in all temperature regimes (Figure 7c). The relative nitrous oxide emissions increased on average 2.5, 2.5 and 2.3 times for 6°C, 8.5°C and 11°C, respectively (Figure 7c), as they are more sensitive to compaction-induced changes in WFPS than changes in temperature (Equation 13). The cumulative nitrate leaching increased with soil compaction by 19%, 14% and 5% for 6°C, 8.5°C and 11°C, respectively (Figure 7d).

4.2.5 | Compaction Impacts for Different Soil Structure Recovery Rate Scenarios

Changes in crop yield and environmental variables were predicted for three different recovery rates including no recovery and full recovery after 5 and 10 years (Figure 9). To illustrate the accumulated effects of soil compaction, we calculated the accumulated (sum of all yearly totals) "losses" for a period of 20 years (corresponding to a generation) after compaction (Figure 10). We tested whether the simulated variables recovered at the rates as the soil structure recovery. For the 5- and 10-years recovery regimes, crop yield recovered to non-compacted values after 5 and 10 years, respectively (Figure 9a). The relative soil organic carbon stocks were slightly affected for the first years after compaction but reduced less than 0.5% when recovery is considered (Figure 9b). Relative nitrous oxide emissions recovered

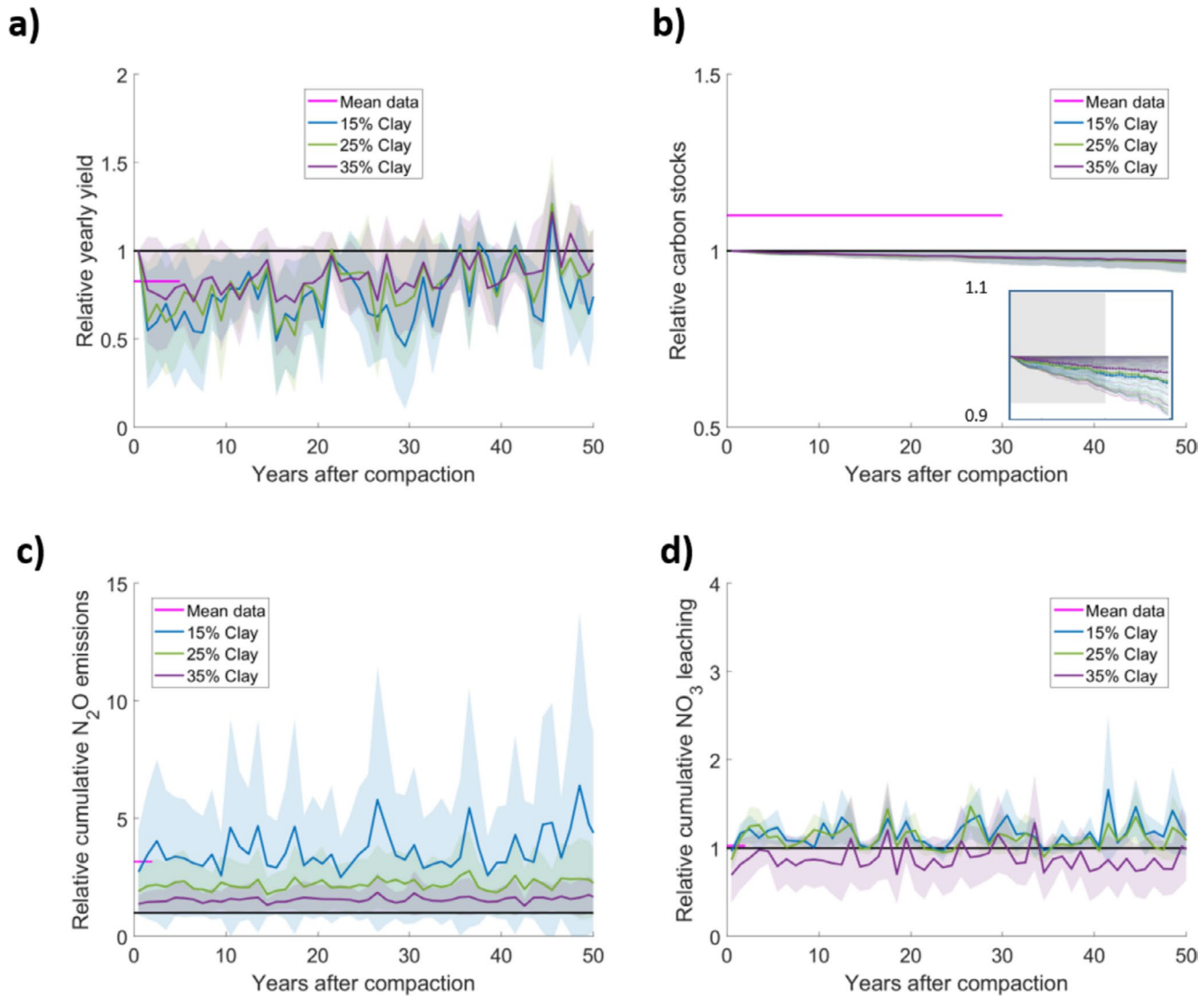

FIGURE 3 | Modelling results of texture-scenarios comparing relative impacts of soil compaction on crop yield (a), soil organic carbon stocks (and zoom in of the entire period for ±5% variations from control) (b), nitrous oxide emissions (c) and nitrate leaching (d). The control line (no compaction = 1) is represented by the black line, the mean values of the literature data are shown by the magenta lines and the shaded area corresponds to the standard deviation range of the literature data. The modelling results for the 25% clay content (green line) represent the base case scenario.

to pre-compaction levels at a rate consistent with recovery regimes, achieving full recovery 7 and 9 years after compaction for the 5- and 10-year recovery regimes, respectively (Figure 9c). Similarly, cumulative nitrate leaching recovered at 5 and 8 years after compaction for the 5- and 10-year recovery regimes, respectively (Figure 9d). In this model, the recovery times of soil functions are not expected to be the same as recovery times prescribed for soil structure properties. Soil function recovery depends not only on the soil properties but also on the budgets of carbon and nutrients, which are disrupted in previous years by the combination of compaction and yearly climates.

Crop yield and carbon stocks are predicted to be diminished by soil compaction and the nitrate leaching and nitrous oxide emissions are increased with compaction when considering an accumulated period of 20-year for all recovery regimes (Figure 10). The losses were maximum in the non-recovery scenario and were predicted to be 21.79 and 0.89 Mg ha^{-1} for yield and carbon stocks, respectively; and nitrogen losses were predicted to be 10.8 and 163.5 kg ha^{-1} for nitrous oxide emissions and nitrate leaching, respectively (Figure 10). Conversely, the losses were minimum in the 5-year recovery scenario and were predicted to be 1.4 and 0.03 Mg ha^{-1} for yield and carbon stocks, respectively; and nitrogen losses were predicted to be 0.9 and 3.7 kg ha^{-1} for nitrous oxide emissions and nitrate leaching, respectively (Figure 10).

5 | Discussion

5.1 | Compaction Decreases Crop Yields

The simulated annual average crop yield was in average 3.2 and 2.3 Mg ha^{-1} for control and compacted in the base case (i.e., without soil structure recovery), respectively. These values are consistent with winter wheat yield in unfertilized soils (Agnolucci and De Lipsis 2020; Burton et al. 2024; Coleman et al. 2017). In

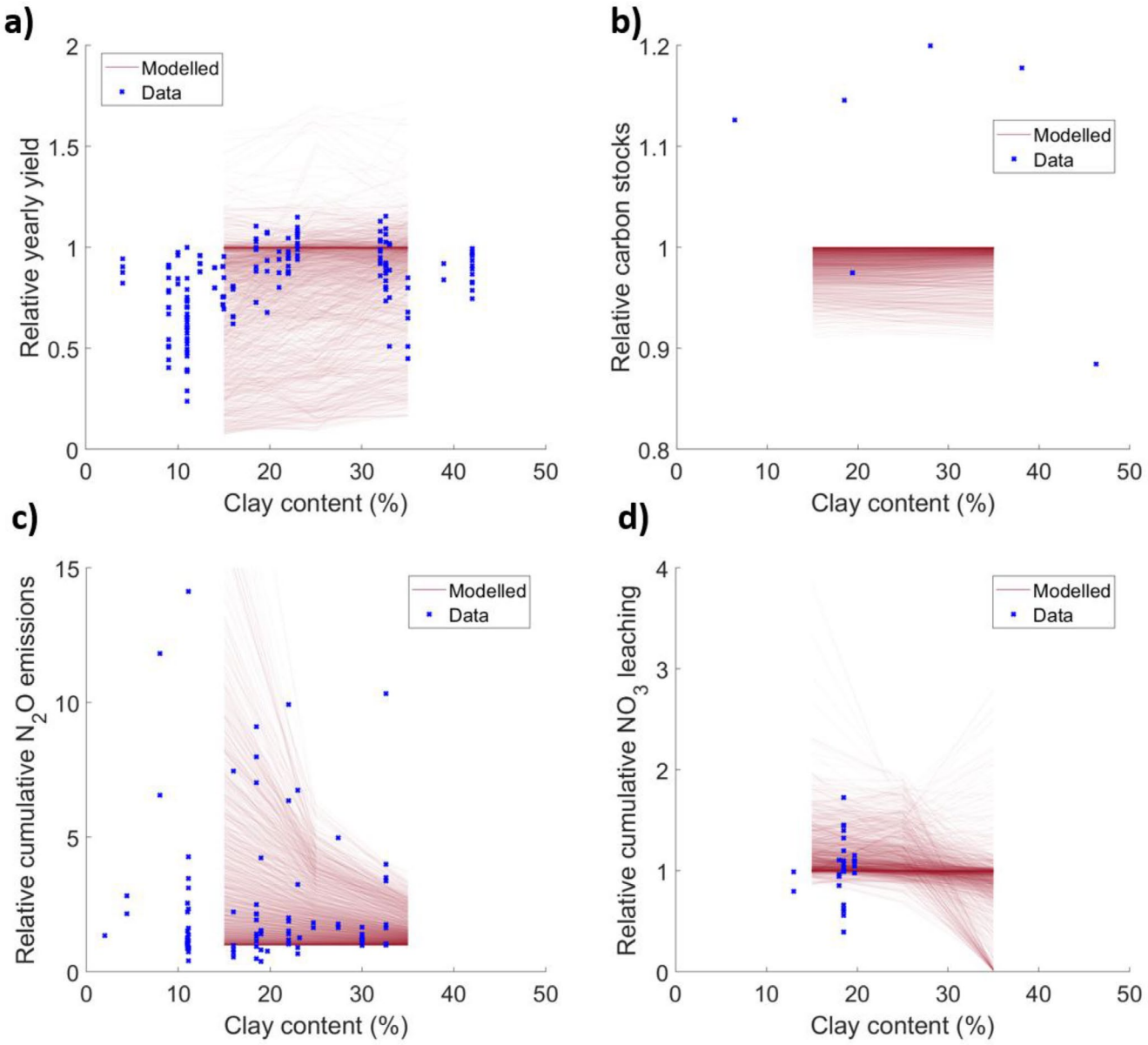

FIGURE 4 | Modelling results of texture-scenarios and literature data (blue dots) comparing relative impacts of soil compaction on crop yield (a), soil organic carbon stocks (b), yearly nitrous oxide emissions (c) and yearly nitrate leaching (d) as a function of clay content. Each modelled curve corresponds to: (i) one compaction level and (ii) one individual year for a period of 50 years after compaction. The literature data are for any time (study dependent) after compaction.

the base case compaction scenarios (Table S5), compaction resulted in an average crop yield decrease of 26%. This decline in crop yield due to compaction aligns with most studies reported in the literature (Figure 3a). The decline is predicted to be similar for different fertilisation rates (Figure S4). In addition, the results show that the water biomass formation factor is similar for both compacted and uncompacted simulations under the low precipitation scenario (Figures S12b and S12c), indicating that water limitation reduces crop yield in both cases and hence minimizes compaction induced losses. Some studies have reported increases in yield in response to compaction for certain years (Håkansson and Reeder 1994; Liu et al. 2022), which is attributed to increased soil moisture that can be beneficial in generally dry years (Liu et al. 2022). The trade-offs between compaction induced reduced percolation and water and nutrient availability depend on pedoclimatic conditions and deserve further investigation.

Literature data suggest that the compaction-induced increase in yields can occur in a wide range of clay contents, which was replicated by the modelling results (Figures 4a–10a). Our modelling results also showed that compacted soils may occasionally show an increase in yield for certain years (Figures 4a, 6a,and 8a), driven by annual fluctuations in temperature and precipitation. Increased yields in certain years could potentially mask the overall negative effects of compaction (Arvidsson and Håkansson 1996). However, when considering the cumulative effects over several years, the long-term consequences of soil compaction become evident, resulting in consistent crop yield losses in all simulated scenarios (Figures S5–S9a and Figure 10a).

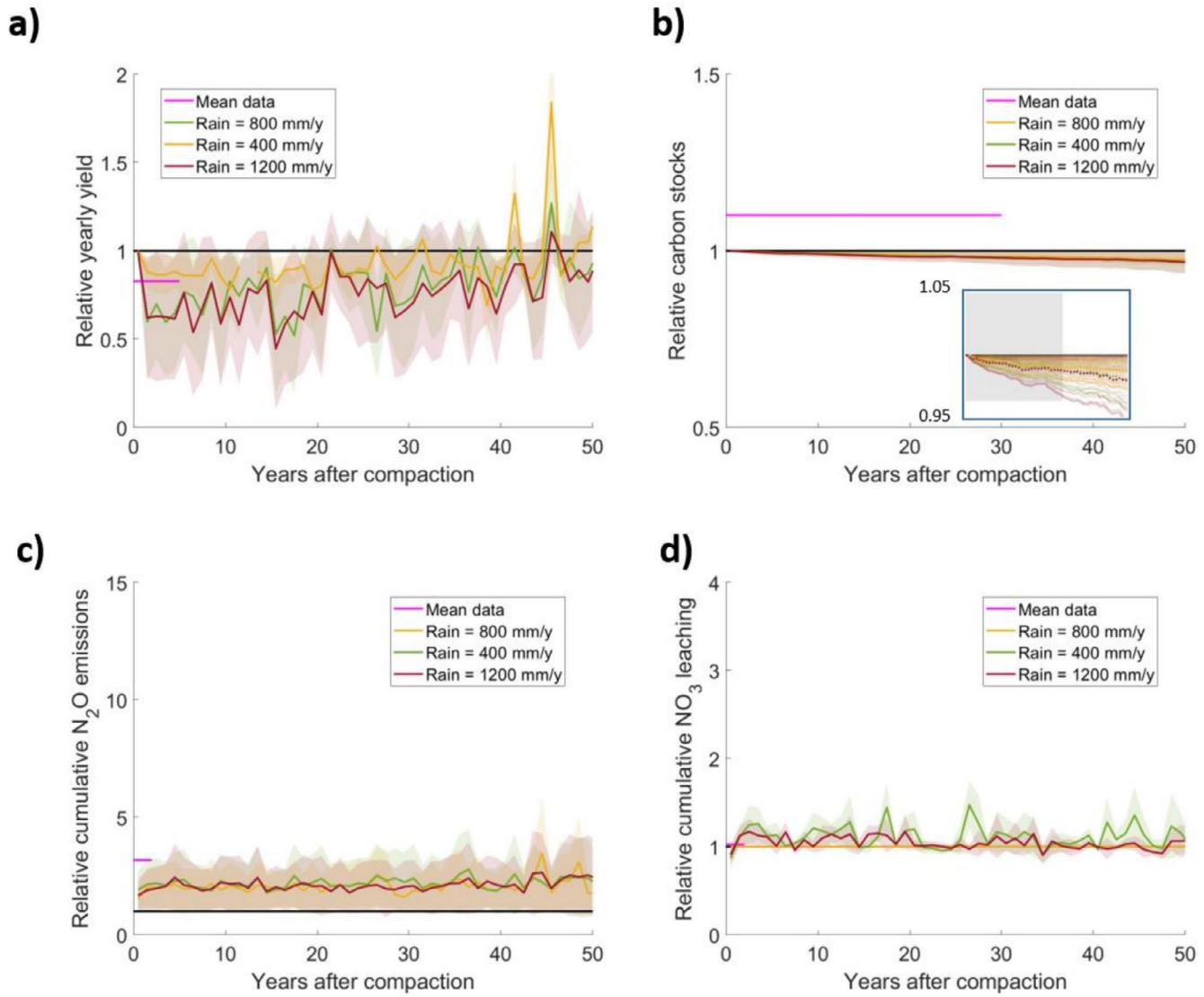

FIGURE 5 | Modelling results of precipitation-scenarios comparing relative impacts of soil compaction on crop yield (a), soil organic carbon stocks (and zoom in of the entire period for ±5% variations from control) (b), nitrous oxide emissions (c) and nitrate leaching (d). The control line (no compaction = 1) is represented by the black line, the mean values of the literature data are reported (magenta line) and the shaded area corresponds to the standard deviation range.

5.2 | Carbon Stocks and Increase or Decrease in Compacted Soils

The model predicted a decrease in carbon stocks for all soil textures, climates, recovery rates and compaction levels (Figures 3b–10b), in contrast to measured data reported in the literature that indicated that compaction can result in soil organic carbon stock increases or decreases (Figure 2b). The model predicted decreases in soil carbon stocks as a result of decreased carbon inputs by plants to the soil. This was caused by the reductions in hydraulic conductivity, which led to persistently higher water-filled pore space in the soil (see Figure S11) that limited the biomass formation through the transpiration reduction factor (Equation 5, Figure S12). The decrease in hydraulic conductivity combined with a compaction-induced increase in root penetration resistance reduced the shoot and root biomass, which comprise soil carbon inputs in the model (Figure S11 in the SI). Yet, mineralisation (i.e., carbon losses by CO_2) was predicted to be higher for non-compacted soil (Figure S13). Hence, modelled changes in soil organic carbon content due to compaction were relatively small for all simulated scenarios (lower than 2 Mg ha^{-1} within a 20-year period, Figure 10b). This also implies that the relative impact of decreased yields in soil carbon losses varies depending on how compaction modifies mineralisation, which would vary depending on pedoclimatic conditions. The modelled effect was similar for different clay contents (Figures 3b and 4b), for different precipitation scenarios (Figures 5b and 6b) and for temperature scenarios (Figures 7b and 8b). A rapid recovery of soil hydraulic properties, with concurrent rapid recovery of the water dynamics, was predicted to maintain soil organic carbon stocks at levels similar as in non-compacted soil (Figure 10b; Figure S9b).

Literature reports of carbon stocks typically focus on the topsoil (Dupla et al. 2024), where carbon may accumulate in compacted soils due to the lateral growth of crop roots promoted by

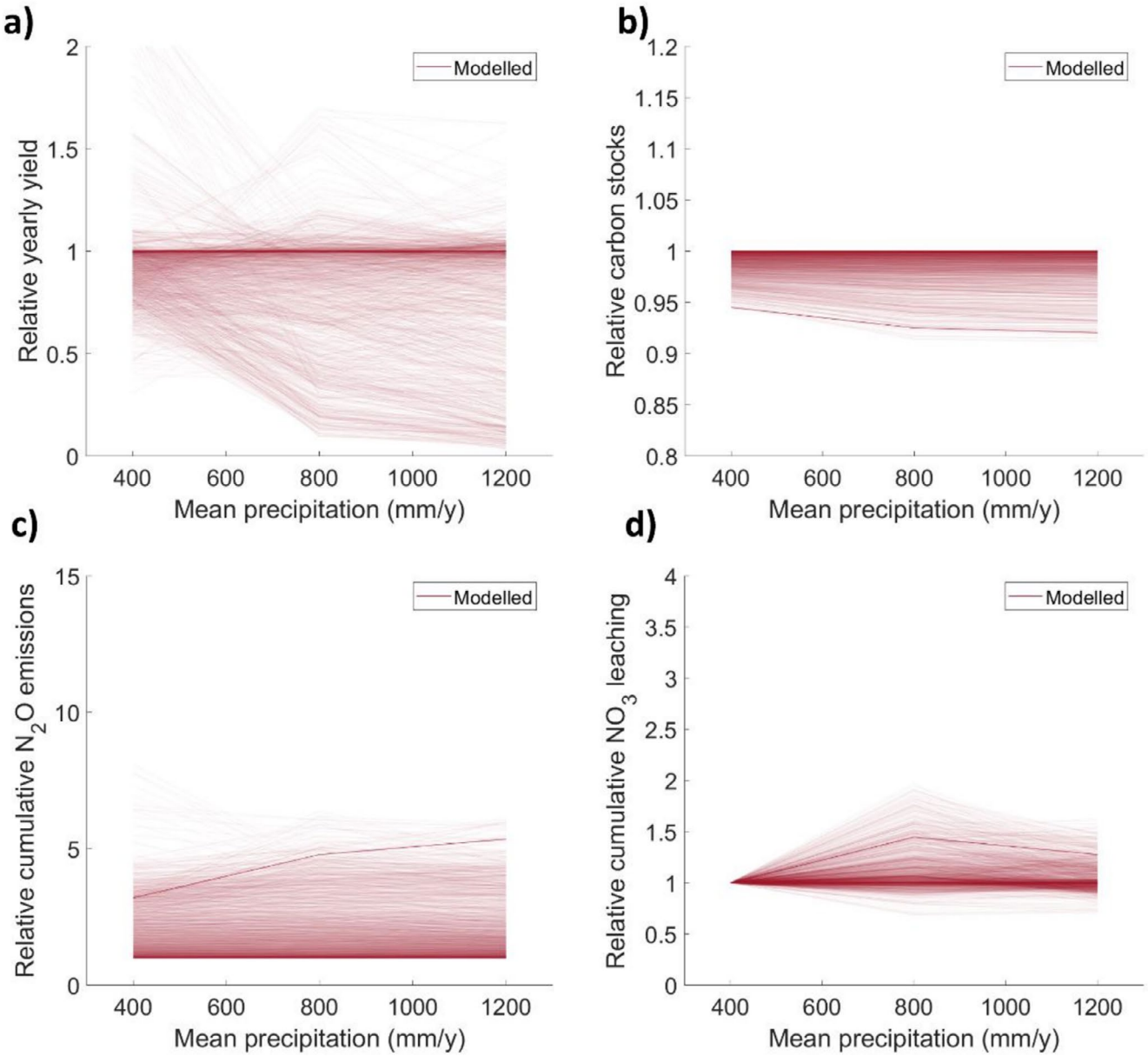

FIGURE 6 | Modelling results of precipitation scenarios comparing relative impacts of soil compaction on crop yield (a), soil organic carbon stocks (b), yearly nitrous oxide emissions (c) and yearly nitrate leaching (d) as a function of mean annual precipitation. Each modelled curve corresponds to all levels of compaction on a given year for the first 50 years after compaction.

increased penetration resistance of the subsoil (Or et al. 2021). Thanks to this, soil organic carbon stocks may be higher in the topsoil for compacted soils but reduced in the subsoil. Our modelling framework is one dimensional and does not consider such lateral root growth and hence is unable to predict the related depth dependent dynamics (Figure S14). In addition, the shoot to root ratio biomass is assumed to be constant in the model. This assumption may not be valid in compacted soils where plants may (have to) invest more into roots (Hoffmann and Jungk 1995; Masle and Passioura 1987), which may result in maintaining the below-ground carbon inputs (i.e., decaying roots) unaffected compared with a non-compacted scenario. Similarly, roots may excrete more mucilage and compaction may result in increased slaughtering of root-cells to decrease friction (Boeuf-Tremblay et al. 1995; Iijima et al. 2000); which could lead to an increase in soil carbon inputs. As predicted, mineralisation of soil organic carbon is another process that may be hindered by compaction due to reduced soil aeration caused by decreased gas transport properties (Asady and Smucker 1989). This reduction may preserve soil organic carbon pools in compacted soils in comparison with non-compacted soils and compaction may also create physical protection for soil carbon in the soil (Monroe et al. 2021). In addition, losses of dissolved soil organic carbon by leaching may play a role in the total carbon stock of compacted soils (Nakhavali et al. 2021). By reducing drainage in some scenarios, soil compaction may prevent carbon losses due to leaching in cases where carbon dissolution is high (Deurer et al. 2012). Finally, certain management practices not accounted for in this model, such as the addition of organic matter amendments, fertilisation, crop rotation and tillage operations may differently impact the dynamics of carbon stocks in compacted and non-compacted soils. Future research should focus

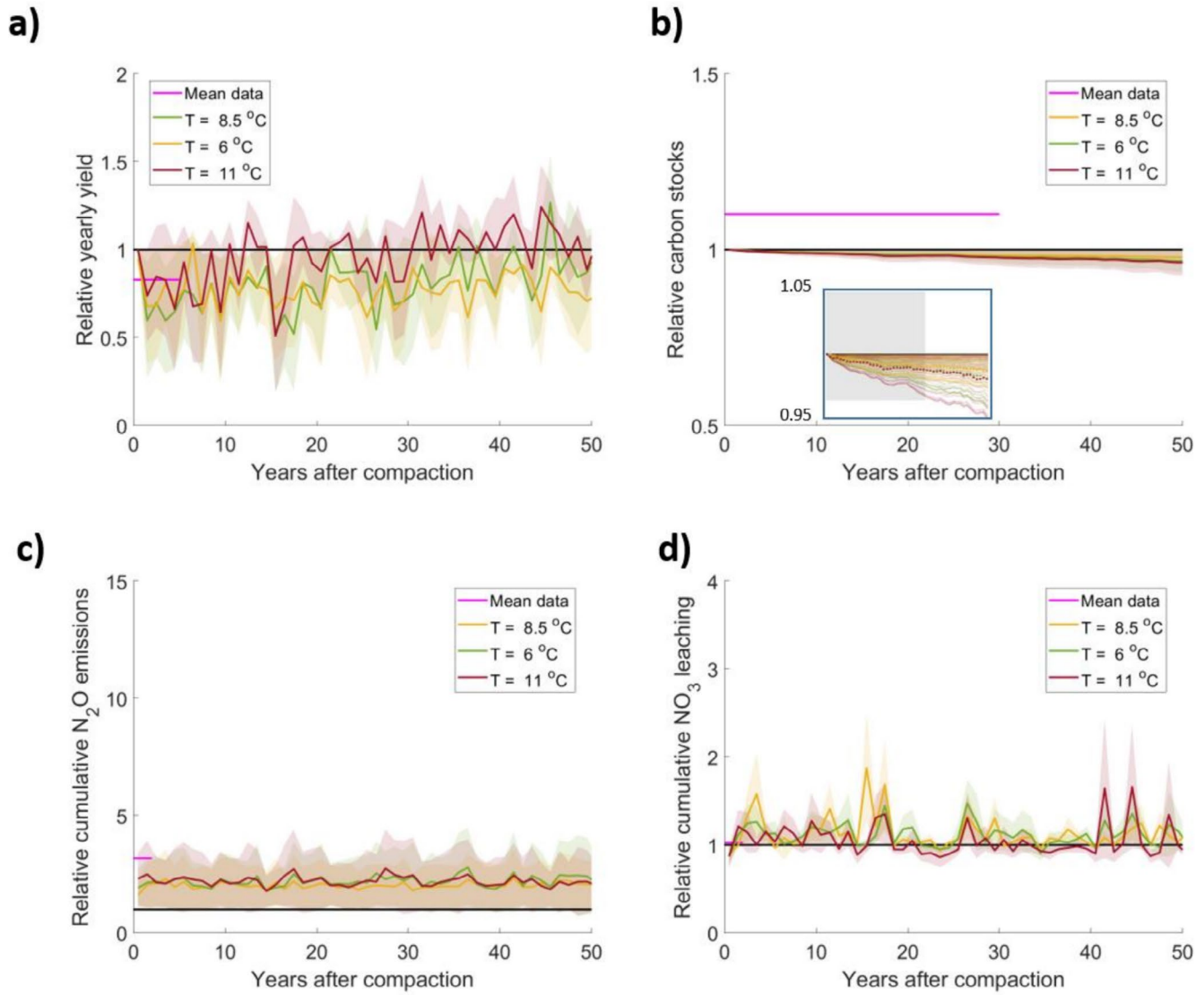

FIGURE 7 | Modelling results of temperature-scenarios comparing relative impacts of soil compaction on crop yield (a), soil organic carbon stocks (and zoom in of the entire period for ±5% variations from control) (b), nitrous oxide emissions (c) and nitrate leaching (d). The control line (no compaction = 1) is represented by the black line, the mean values of the literature data are reported (magenta line) and the shaded area corresponds to the standard deviation range.

on understanding the relative effects of the above-mentioned mechanisms (reduction of root biomass, reduction of mineralisation, increase in amounts of mucilage, decrease in dissolved carbon leaching, increased carbon protection) on soil carbon stocks of compacted soils by establishing long-term experiments under different soil types and climates (and/or complementing with chrono-sequence experiments) targeting the monitoring of carbon losses.

5.3 | Compaction Increases Nitrous Oxide Emissions

The strong impact of soil compaction on soil water dynamics is believed to be the most dominant factor controlling nitrous oxide emissions from compacted soils (Hu et al. 2021). Denitrification by anaerobic microbial activity is very sensitive to compaction-induced increases in water filled pore space, caused by inflicted reductions of pore space and water and gas transport properties (Pulido-Moncada et al. 2022) that result in slow water movement and low oxygen diffusion (Figures S11 and S15).

The modelling framework used in this study focused on representing soil compaction impacts on soil hydraulic properties and water dynamics. Consequently, the modelling results agreed with most literature reports (Figure 4c), predicting an increase in nitrous oxide emissions for all soil textures, climates, soil structure recovery rates and compaction levels (Figures 3c–10c). Relative nitrous oxide emissions decreased with clay content (Figure 4c), yet, the model predicted absolute accumulated losses of nitrous oxide emissions to increase with increasing clay content (Figure S6c) because nitrous oxide emissions are considerably higher for clayey soils. This is because the rate of change of the denitrification factor, which depends on water filled pore space (derivative of Equation 14), is higher for lower water content ranges, which are more likely in soils with lower clay

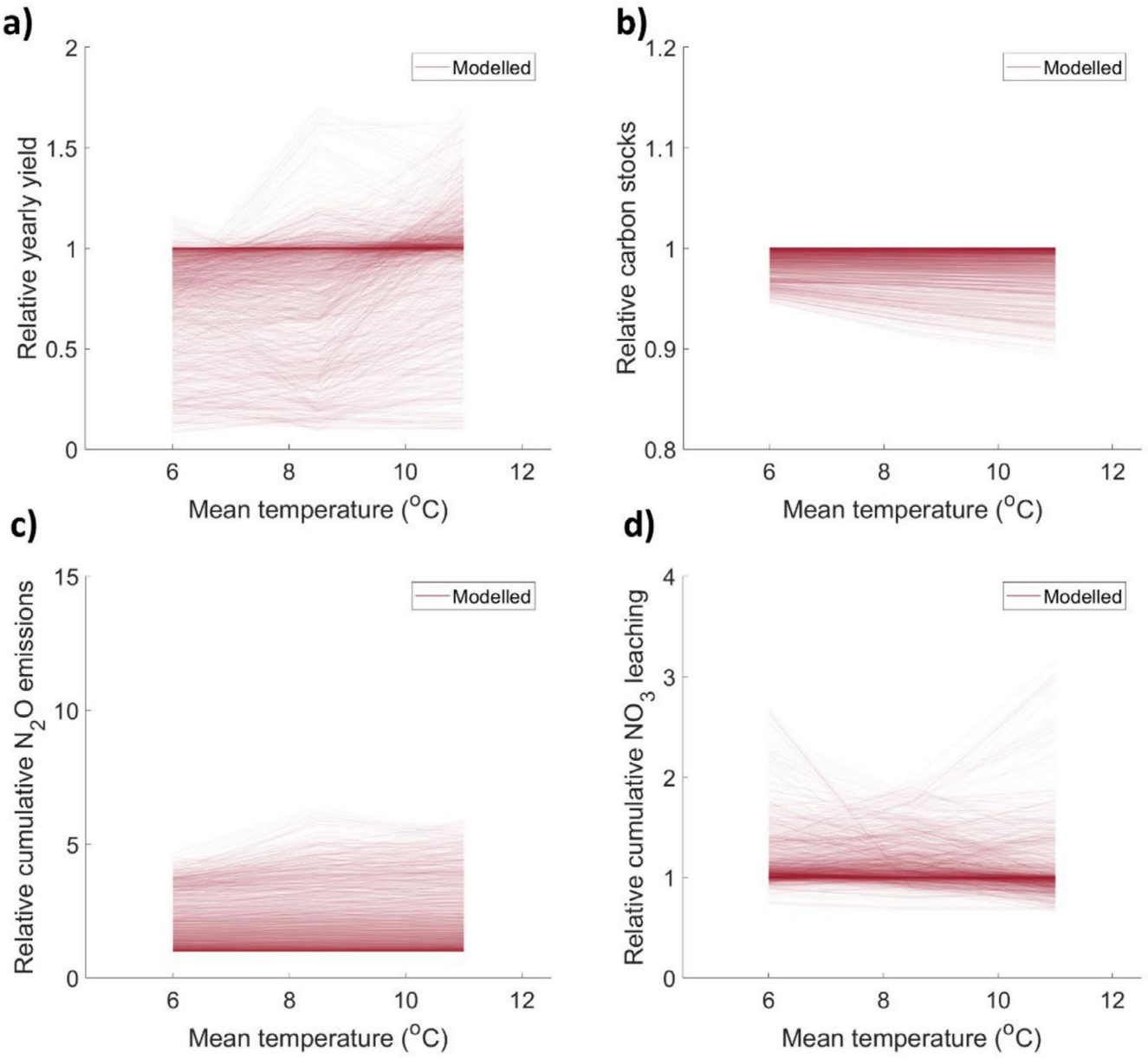

FIGURE 8 | Modelling results of temperature-scenarios comparing relative impacts of soil compaction on crop yield (a), soil organic carbon stocks (b), yearly nitrous oxide emissions (c) and yearly nitrate leaching (d) as a function of mean annual precipitation. Each modelled curve corresponds to all levels of compaction on a given year for the first 50 years after compaction.

contents (i.e., lower water content at field capacity). The variations in precipitation and temperature regimes did not have a strong effect on nitrous oxide emissions and all soil structure recovery regimes produced a clear reduction of the relative nitrous oxide emissions (Figure 9c), although there were accumulated losses irrespective of the recovery rate (Figure 10c). In general, the model successfully reproduced the ranges and trends of compaction-induced increases in nitrous oxide emissions reported in the literature (Figure 2).

Despite the relatively good agreement between simulated nitrous oxide emissions and the literature evidence for compacted soils, these results should be taken carefully. Not all the processes involved in nitrous oxide emissions were considered in the model, such as those related to the demand of oxygen in soil organic matter decomposition (that similarly create anaerobic conditions) or the seasonal changes in microbial community sizes, diversity and function. The accumulated emissions were simulated to increase with compaction for all systems regardless of climate, soil type and recovery regime. Yet, they are strongly reduced when recovery is considered, even for slow recovery scenarios, which highlights the relevance of avoiding recompaction and allowing recovery.

5.4 | Does Compaction Exacerbate Nitrate Leaching?

The strong impact of soil compaction on soil water dynamics is considered the primary factor controlling nitrate leaching (Yi et al. 2022). While the reduction of soil water transport properties in severely compacted soils may prevent leaching, limited

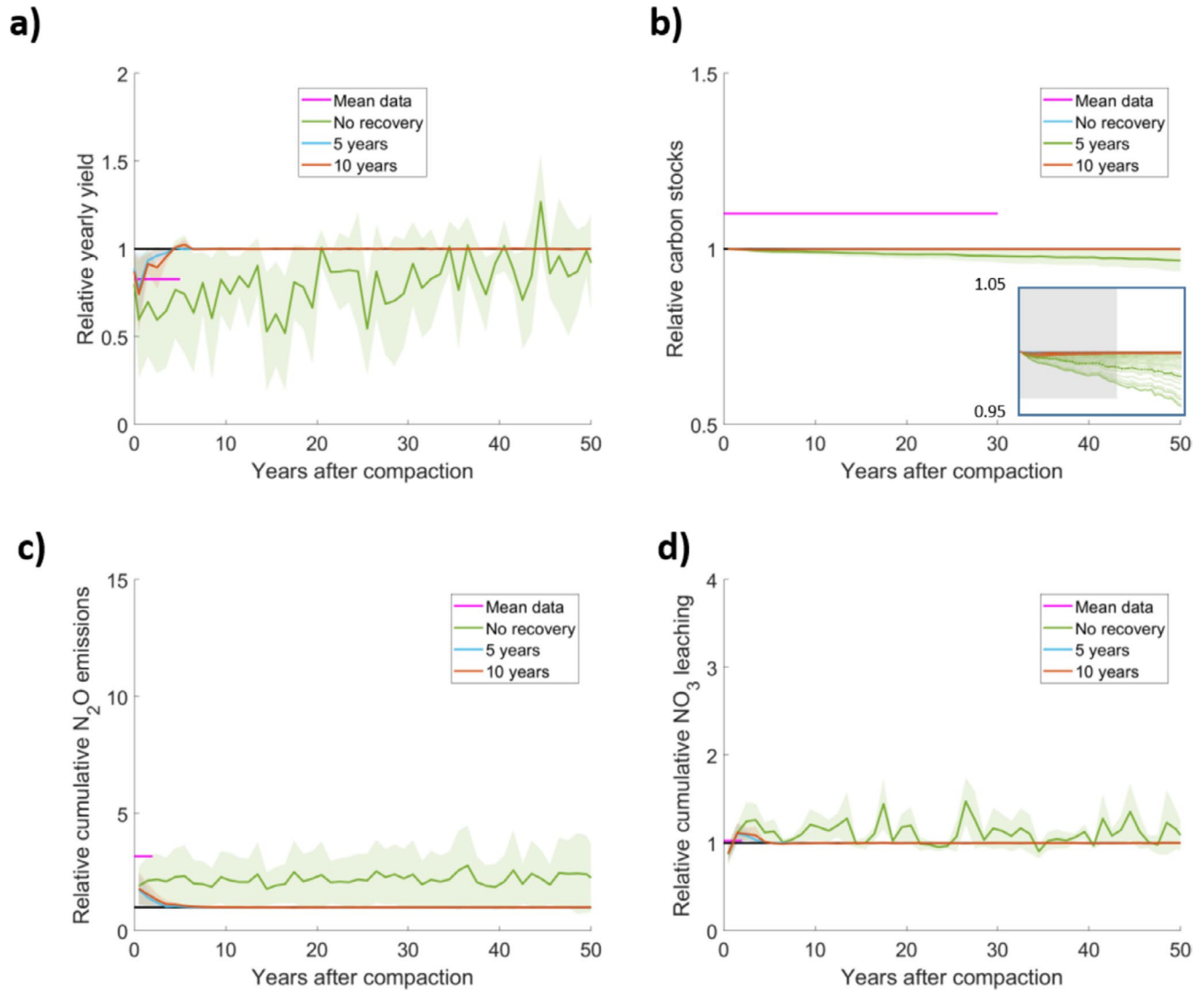

FIGURE 9 | Modelling results of recovery scenarios comparing relative impacts of soil compaction on crop yield (a), soil organic carbon stocks (and zoom in of the entire period for −+5% variations from control) (b), nitrous oxide emissions (c) and nitrate leaching (d). The control line (no compaction = 1), the mean values of the data are reported and the shaded area corresponds to the standard deviation range.

root volumes due to increased penetration resistances can facilitate leaching of inaccessible nitrate (Strock et al. 2022). The overall mechanisms for nitrate leaching involve the interactions between soil hydraulic properties controlling water flow, precipitation and evapotranspiration that promote and prevent downward movement, respectively. Similarly, soil penetration resistance plays a role in nitrate leaching as it determines the root distribution in the soil profile and hence nutrient and water accessibility and uptake by roots. The relative contribution of these system characteristics varies for different scenarios and hence the predicted nitrate leaching is scenario-dependent. In the base case, the model predicted a decrease in root length due to compaction in all depths. On average, root length decrease was about 30% (see Figure S12b) and decreases were highest for the 0.23–0.46 m soil layer. The model predicted an increase in nitrate leaching for soils with the two lowest clay content (15% and 25%), irrespective of climate, soil structure recovery rate and compaction level (Figures 3d–10d). However, the nitrate leaching was predicted to be similar or lower in compacted soil for a soil with 35% clay content (Figure 4d) for which already limited water transport properties of the soil matrix control water flow (Figures S3e and S11a). This resulted in a small net accumulated leaching, with no clear trend of increase or decrease between the compacted and non-compacted soils (Figure S6d).

Although nitrate leaching was predicted to be increased by compaction in most years, the predicted range in nitrate leaching for low clay contents was consistent with literature reports (Figure 4d). Unlike nitrous oxide emissions, precipitation and temperature scenarios had clear effects on nitrate leaching (Figures 6d and 8d). Nitrate leaching may increase or decrease due to compaction for a particular year, but the modelling results predicted accumulated losses to always be higher for compacted soils in the long term (Figures 10d and S6d) even when soil structure recovery was considered (Figure 10d). In addition to annual mean precipitation and temperature, nitrate leaching is dependent on fertilisation application rates and timing (Figure S4).

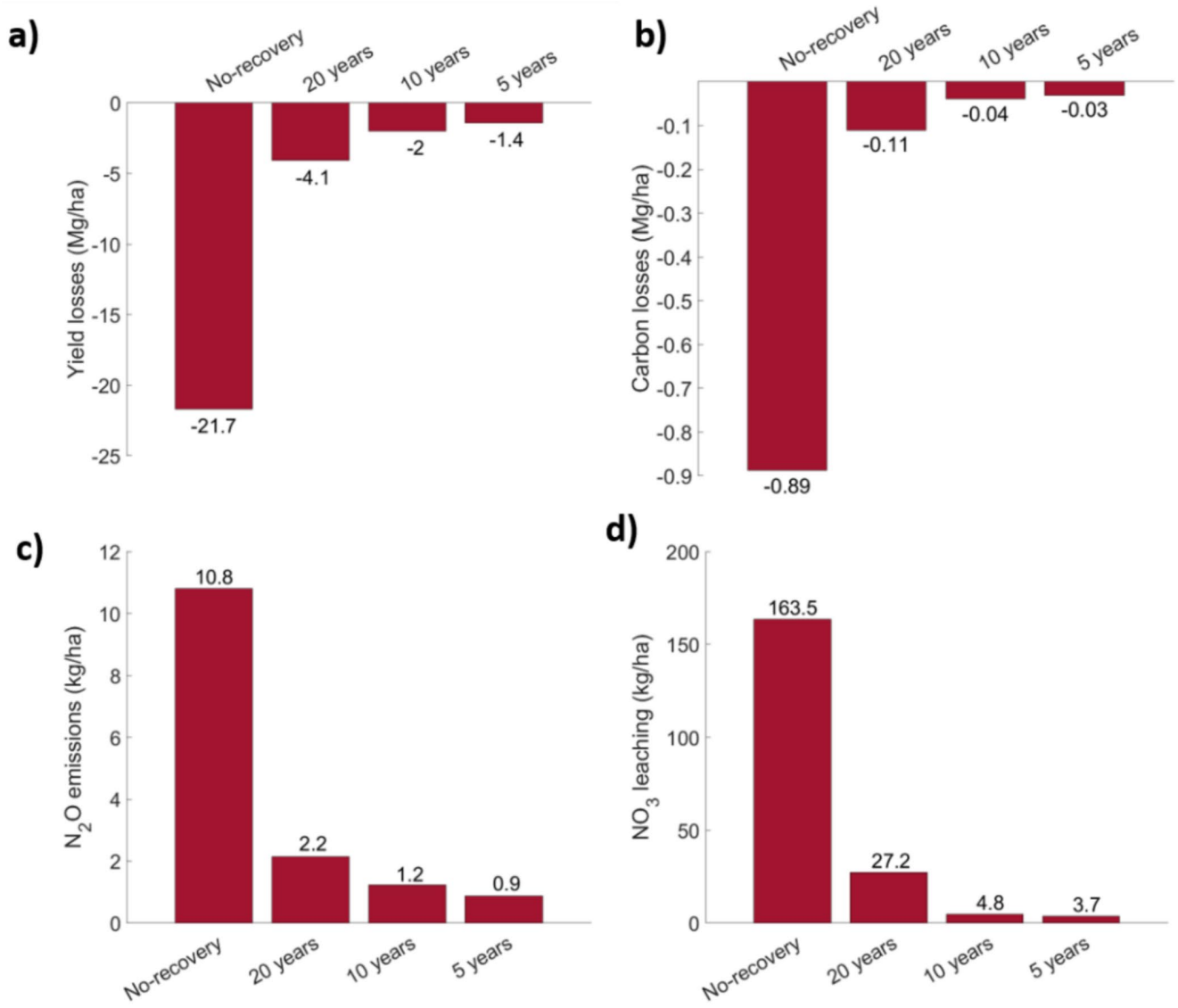

FIGURE 10 | Modelling results of the difference between no-compacted–compacted of total crop yield for 20 years after compaction (a), soil organic carbon stocks at 20 years after compaction (b), accumulated nitrous oxide emissions in 20 years after compaction (c) and accumulated nitrate leaching 20 years after compaction (d) for the different recovery rates considered in this study. These results correspond to a wheel load of 8 Mg.

The generally good agreement between modelling results and literature reports (Figure 4d) suggest that the model captures differences in soil water flow between compacted and not compacted soils. Yet, literature data remain limited and the modelling results must be taken carefully. The model does not capture certain properties and processes that are impacted by compaction and relevant for nitrate leaching. These processes are similar to those influencing carbon cycling. For example, soil compaction may promote lateral growth of crop roots making nutrients at deeper depths inaccessible and prone to leaching. Also, leaching may be increased by preferential flow occurring in isolated macropores created by mesofauna in compacted soils, which could trigger nitrate leaching especially directly after fertilisation events (for liquid fertilizers) and in heavy rainfall climates. The dual-porosity water flow model considered here (Equations 3 and 4) does not simulate preferential flow (i.e., high values of hydraulic conductivity by the activation of the macroporosity only occur after the soil matrix is fully saturated) and assumed that compaction did not change the soil matrix, which may lead to underestimation of nitrate leaching for high precipitation scenarios. Because of this, the simulated differences in nitrate leaching are produced by interactions between the water flow and the crop model. Root water and nitrate uptake are simulated to be higher in the non-compacted soil. In comparison, this leads to higher water filled pore space (Figure S11) and hence typically higher hydraulic conductivities in the compacted soils and more availability of unused nitrate for leaching. Finally, nitrate leaching depends also on microbial activity and composition controlling nitrogen dynamics in the soil, which are further affected by compaction (Breland and Hansen 1996). All these interacting processes further highlight the complexity of predicting nitrate leaching in structured soils (Holbak et al. 2022) and under the presence of vegetation. Yet, our modelling approach may serve as a starting point and provide simulations results that help optimising fertilisation times and rates in compacted soils (similarly to the approach by Coleman et al. 2017).

5.5 | Limitations and Outlook

The soil-structure based modelling framework presented here successfully simulated most compaction-induced trends in soil (dis)services, offering valuable insights on the negative effects of soil compaction on crop yield and environment under a range of pedo-climatic conditions. Yet, the work presented here has several shortcomings that can be summarized as: (1) limitations related to the simulation of soil deformation due to compaction and impact soil properties, (2) simplifications on the spatial domain comprising one-dimensional representation of processes that can in fact be impacted by 3D heterogeneity, as well as the limited vertical discretisation and representation of spatial heterogeneity of soil physical properties, (3) simplification, lack of consideration, or reliance on calibrated empirical models to represent certain soil physical, chemical and biological processes in the model, (4) uncertainty on how water retention and transport properties vary as a function of soil texture and (5) lack of data to validate modelling predictions, (6) and lack of consideration of diverse management strategies (fertilisation, crop rotation, organic amendments). These are not specific for this modelling work but a limitation of all agroecosystem modelling efforts (Vereecken et al. 2022). In fact, our work presents an advance by explicitly representing management induced soil structural changes in agroecosystem models, which is highly relevant yet rarely included (Jarvis et al. 2024; König et al. 2023; Romero-Ruiz et al. 2024).

Overcoming the abovementioned difficulties is challenging and outside the scope of this work. The modelling results presented in this work offer clues of mechanistic explanation on how processes that are currently considered in agroecosystem modelling are impacted by compaction and how this impacts crop yields and the environment. The model successfully reproduced trends of relative crop yields, nitrous oxide emissions and nitrate leaching and partially reproduced trends on relative carbon stocks. We believe that despite the simplifications made, this is a first step for accounting for effects of management on soil physical properties that are commonly overseen when modelling agroecosystems. Future modelling efforts will be advocated where detailed soil, weather and management data are available to calibrate and validate model predictions, improving representation of soil processes such as water flow and microbial activity, conducting thresholds and sensitivity analysis over extensive soil types and climate to investigate the links between compaction induced changes in soil functioning; and coupling this model with landscape modelling approaches that represent spatial variability of soil compaction at the field scale and its response to field traffic patterns (Duttmann et al. 2022; Romero-Ruiz, Rivero, et al. 2023). In addition, we also need to advance our quantitative knowledge of how compaction affects relevant soil properties (e.g., soil pore size distribution, pore connectivity and continuity) and microbial community functioning, which can then be implemented in models. Altogether, these advances have the potential of guiding recommendations practitioners to avoid soil function loss according to their specific pedoclimatic conditions (avoiding blanket recommendations). This can be done by integrating the model into a modelling framework considering soil maps (Poggio et al. 2021) and climate projection maps (Eyring et al. 2016) to model soil compaction induced losses in soil functions across European pedoclimatic conditions.

6 | Conclusions

In this work, we used a mechanistic modelling framework to assess the impacts and trends of soil compaction in crop yield, carbon stocks, nitrous oxide emissions and nitrate leaching for different clay contents, precipitation, temperature and recovery scenarios. Literature data suggested that soil compaction: (1) can either increase or decrease carbon stocks in the soil, (2) increases nitrous oxide emissions, (3) decreases crop yields and (4) can either increase or decrease nitrate leaching. The simulations compared favourably with these data, except for carbon stocks, for which only decreases where predicted. The results suggest that the impact of soil compaction on soil water dynamics, a central process in the used modelling framework, plays a prominent role in the resulting changes in soil (dis)services. Overall, the model predictions suggest that long-term effects of soil compaction on crop productivity and environment are negative, even if there are some years with positive effects (e.g., increased crop yield). In a single scenario consisting a severe soil compaction event in a loamy soil (the most common soil type in Europe), soil compaction was predicted to induced reductions in crop yield and carbon stocks were predicted to be 16 and 1 $Mg\,ha^{-1}$; and nitrous oxide emissions and nitrate leaching were predicted to increase by 10 and 163 $kg\,ha^{-1}$ in a 20-year period.

By systematically presenting soil compaction impacts on soil properties and processes, this study offers a first step for understanding how soil compaction impacts soil (dis)services (1) for different pedoclimatic conditions and (2) in the long-term by assessing accumulated effects less sensitive to local short-term climate conditions. Future work could use this modelling framework to estimate soil compaction-induced impacts on the environment and yield at a country or continental scale, its contribution to agricultural greenhouse gases production, potential economic losses and the potential of prevention or remediation strategies to ameliorate such adverse impacts.

Author Contributions

Alejandro Romero-Ruiz: writing – review and editing, conceptualization, data curation, methodology, investigation. **Lorena Chagas Torres:** writing – review and editing, investigation, methodology. **Mathieu Lamandé:** conceptualization, investigation, writing – review and editing, project administration, funding acquisition. **Michael Kuhwald:** investigation, writing – review and editing, methodology. **Thomas Keller:** conceptualization, investigation, funding acquisition, writing – review and editing, project administration.

Acknowledgements

This work was funded under the European Joint Program for SOIL (EJP SOIL), subproject SoilCompaC, which has received funding from the European Union's Horizon 2020 research and innovation programme: Grant agreement No 86269. We gratefully acknowledge the Agroecosystem Modelling group in Rothamsted Research for making the RLM available. The authors are grateful to two anonymous reviewers and the Editors for their valuable comments that helped

improve the quality of this manuscript. Open access publishing facilitated by Agroscope, as part of the Wiley - Agroscope agreement via the Consortium Of Swiss Academic Libraries.

Funding

This work was supported by HORIZON EUROPE Innovative Europe.

Data Availability Statement

The data that support the findings of this study are available from the corresponding author upon reasonable request.

References

Agnolucci, P., and V. De Lipsis. 2020. "Long-Run Trend in Agricultural Yield and Climatic Factors in Europe." *Climatic Change* 159: 385–405.

Arvidsson, J., and I. Håkansson. 1996. "Do Effects of Soil Compaction Persist After Ploughing? Results From 21 Long-Term Field Experiments in Sweden." *Soil and Tillage Research* 39, no. 3: 175–197. https://doi.org/10.1016/S0167-1987(96)01060-4.

Asady, G. H., and A. J. M. Smucker. 1989. "Compaction and Root Modifications of Soil Aeration." *Soil Science Society of America Journal* 53, no. 1: 251–254.

Azam, G., C. D. Grant, R. S. Murray, I. K. Nuberg, and R. K. Misra. 2014. "Comparison of the Penetration of Primary and Lateral Roots of Pea and Different Tree Seedlings Growing in Hard Soils." *Soil Research* 52, no. 1: 87–96.

Berisso, F. E., P. Schjnning, T. Keller, et al. 2012. "Persistent Effects of Subsoil Compaction on Pore Size Distribution and Gas Transport in a Loamy Soil." *Soil and Tillage Research* 122: 42–51.

Bi, D., M. Dix, S. Marsland, et al. 2020. "Configuration and Spin-Up of ACCESS-CM2, the New Generation Australian Community Climate and Earth System Simulator Coupled Model." *Journal of Southern Hemisphere Earth Systems Science* 70, no. 1: 225–251.

Bieger, K., J. G. Arnold, H. Rathjens, et al. 2017. "Introduction to SWAT+, a Completely Restructured Version of the Soil and Water Assessment Tool." *JAWRA Journal of the American Water Resources Association* 53, no. 1: 115–130.

Blackwell, P. S., M. A. Ward, R. N. Lefevre, and D. J. Cowan. 1985. "Compaction of a Swelling Clay Soil by Agricultural Traffic; Effects Upon Conditions for Growth of Winter Cereals and Evidence for Some Recovery of Structure." *Journal of Soil Science* 36, no. 4: 633–650.

Boeuf-Tremblay, V., S. Plantureux, and A. Guckert. 1995. "Influence of Mechanical Impedance on Root Exudation of Maize Seedlings at Two Development Stages." *Plant and Soil* 172: 279–287.

Boons-Prins, E. R., G. H. J. De Koning, and C. A. Van Diepen. 1993. "Crop-Specific Simulation Parameters for Yield Forecasting Across the European Community." CABO-DLO and SC-DLO.

Breland, T. A., and S. Hansen. 1996. "Nitrogen Mineralization and Microbial Biomass as Affected by Soil Compaction." *Soil Biology and Biochemistry* 28, no. 4: 655–663.

Burton, A., L. L. Hner, N. Schaad, et al. 2024. "Evaluating Nitrogen Fertilization Strategies to Optimize Yield and Grain Nitrogen Content in Top Winter Wheat Varieties Across Switzerland." *Field Crops Research* 307: 109251.

Carsel, R. F., and R. S. Parrish. 1988. "Developing Joint Probability Distributions of Soil Water Retention Characteristics." *Water Resources Research* 24, no. 5: 755–769.

Chamen, T. W. C., A. P. Moxey, W. Towers, B. Balana, and P. D. Hallett. 2015. "Mitigating Arable Soil Compaction: A Review and Analysis of Available Cost and Benefit Data." *Soil and Tillage Research* 146, no. pt: 10–25.

Coleman, K., and D. Jenkinson. 2014. "RothC—A Model for the Turnover of Carbon in Soil: Model Description and Users Guide." Lawes Agricultural Trust, Harpenden, UK. Updated June 2014.

Coleman, K., and D. S. Jenkinson. 1996. "RothC-26.3-A Model for the Turnover of Carbon in Soil." In *Evaluation of Soil Organic Matter Models: Using Existing Long-Term Datasets*, 237–246. Springer.

Coleman, K., S. E. Muhammed, A. E. Milne, et al. 2017. "The Landscape Model: A Model for Exploring Trade-Offs Between Agricultural Production and the Environment." *Science of the Total Environment* 609: 1483–1499.

Colombi, T., L. Chagas, A. Walter, and T. Keller. 2018. "Feedbacks Between Soil Penetration Resistance, Root Architecture and Water Uptake Limit Water Accessibility and Crop Growth—A Vicious Circle." *Science of the Total Environment* 626: 1026–1035.

Deurer, M., K. Mller, I. Kim, et al. 2012. "Can Minor Compaction Increase Soil Carbon Sequestration? A Case Study in a Soil Under a Wheel-Track in an Orchard." *Geoderma* 183: 74–79.

Dupla, X., E. Bonvin, C. Deluz, et al. 2024. "Are Soil Carbon Credits Empty Promises? Shortcomings of Current Soil Carbon Quantification Methodologies and Improvement Avenues." *Soil Use and Management* 40, no. 3: e13092.

Durner, W. 1994. "Hydraulic Conductivity Estimation for Soils With Heterogeneous Pore Structure." *Water Resources Research* 30, no. 2: 211–223.

Duttmann, R., K. Augustin, J. Brunotte, and M. Kuhwald. 2022. "Modeling of Field Traffic Intensity and Soil Compaction Risks in Agricultural Landscapes." In *Advances in Understanding Soil Degradation*, edited by E. Saljnikov, L. Mueller, A. Lavrishchev, et al., 313–331. Springer International Publishing. https://doi.org/10.1007/978-3-030-85682-3_14.

Eyring, V., S. Bony, G. A. Meehl, et al. 2016. "Overview of the Coupled Model Intercomparison Project Phase 6 (CMIP6) Experimental Design and Organization." *Geoscientific Model Development* 9, no. 5: 1937–1958. https://doi.org/10.5194/gmd-9-1937-2016.

Feddes, R. A. 1978. "Simulation of Field Water Use and Crop Yield." In *Simulation of Plant Growth and Crop Production*, edited by F. W. T. Penning de Vries and H. H. van Laar, 194–209. Pudoc.

Gao, W., W. R. Whalley, Z. Tian, J. Liu, and T. Ren. 2016. "A Simple Model to Predict Soil Penetrometer Resistance as a Function of Density, Drying and Depth in the Field." *Soil and Tillage Research* 155: 190–198. https://doi.org/10.1016/j.still.2015.08.004.

Gerwitz, A., and E. Page. 1974. "An Empirical Mathematical Model to Describe Plant Root Systems." *Journal of Applied Ecology* 11: 773–781.

Ghezzehei, T. A., and D. Or. 2001. "Rheological Properties of Wet Soils and Clays Under Steady and Oscillatory Stresses." *Soil Science Society of America Journal* 65, no. 3: 624–637.

Godwin, D. C., and C. Allan Jones. 1991. "Nitrogen Dynamics in Soi-Plant Systems." In *Modeling Plant and Soil Systems*, 287–321. John Wiley & Sons, Ltd.

Goulding, K. W. T., N. J. Bailey, N. J. Bradbury, et al. 1998. "Nitrogen Deposition and Its Contribution to Nitrogen Cycling and Associated Soil Processes." *New Phytologist* 139, no. 1: 49–58.

Håkansson, I., and J. Lipiec. 2000. "A Review of the Usefulness of Relative Bulk Density Values in Studies of Soil Structure and Compaction." *Soil and Tillage Research* 53, no. 2: 71–85.

Håkansson, I., and R. C. Reeder. 1994. "Subsoil Compaction by Vehicles With High Axle Load—Extent, Persistence and Crop Response." *Soil and Tillage Research* 29, no. 2: 277–304.

Hamza, M. A., and W. K. Anderson. 2005. "Soil Compaction in Cropping Systems: A Review of the Nature, Causes and Possible Solutions." *Soil and Tillage Research* 82, no. 2: 121–145.

Heller, O., C. D. Bene, P. Nino, et al. 2024. "Towards Enhanced Adoption of Soil-Improving Management Practices in Europe." *European Journal of Soil Science* 75, no. 2: e13483.

Hernandez-Ramirez, G., R. Ruser, and D.-G. Kim. 2021. "How Does Soil Compaction Alter Nitrous Oxide Fluxes? A Meta-Analysis." *Soil and Tillage Research* 211: 105036.

Hoffmann, C., and A. Jungk. 1995. "Growth and Phosphorus Supply of Sugar Beet as Affected by Soil Compaction and Water Tension." *Plant and Soil* 176: 15–25.

Holbak, M., P. Abrahamsen, and E. Diamantopoulos. 2022. "Modeling Preferential Water Flow and Pesticide Leaching to Drainpipes: The Effect of Drain-Connecting and Matrix-Terminating Biopores." *Water Resources Research* 58, no. 7: e2021WR031608.

Hu, W., J. Drewry, M. Beare, A. Eger, and K. Mller. 2021. "Compaction Induced Soil Structural Degradation Affects Productivity and Environmental Outcomes: A Review and New Zealand Case Study." *Geoderma* 395: 115035.

Iijima, M., B. Griffiths, and A. G. Bengough. 2000. "Sloughing of Cap Cells and Carbon Exudation From Maize Seedling Roots in Compacted Sand." *New Phytologist* 145, no. 3: 477–482.

Jarvis, L., J. Rosenfeld, P. C. Gonzalez-Espinosa, and E. C. Enders. 2024. "A Process Framework for Integrating Stressor-Response Functions Into Cumulative Effects Models." *Science of the Total Environment* 906: 167456.

Keller, T., T. Colombi, S. Ruiz, et al. 2017. "Long-Term Soil Structure Observatory for Monitoring Post-Compaction Evolution of Soil Structure." *Vadose Zone Journal* 16, no. 4: 1–16.

Keller, T., and D. Or. 2022. "Farm Vehicles Approaching Weights of Sauropods Exceed Safe Mechanical Limits for Soil Functioning." *Proceedings of the National Academy of Sciences* 119, no. 21: e2117699119.

König, S., U. Weller, B. Betancur-Corredor, et al. 2023. "BODIUM—A Systemic Approach to Model the Dynamics of Soil Functions." *European Journal of Soil Science* 74, no. 5: e13411.

Li, K. Y., R. De Jong, and J. B. Boisvert. 2001. "An Exponential Root-Water-Uptake Model With Water Stress Compensation." *Journal of Hydrology* 252, no. 1–4: 189–204.

Liu, H., T. Colombi, O. Jäck, T. Keller, and M. Weih. 2022. "Effects of Soil Compaction on Grain Yield of Wheat Depend on Weather Conditions." *Science of the Total Environment* 807: 150763.

Masle, J., and J. B. Passioura. 1987. "The Effect of Soil Strength on the Growth of Young Wheat Plants." *Functional Plant Biology* 14, no. 6: 643–656.

Meurer, K., J. Barron, C. Chenu, et al. 2020. "A Framework for Modelling Soil Structure Dynamics Induced by Biological Activity." *Global Change Biology* 26, no. 10: 5382–5403.

Michli, E., P. Schad, O. Spaargaren, D. Dent, and F. Nachtergaele. 2006. *World Reference Base for Soil Resources: A Framework for International Classification, Correlation and Communication*. FAO (Food and Agriculture Organization).

Monroe, P. H. M., P. A. B. Barreto-Garcia, W. T. Barros, F. G. R. B. de Oliveira, and M. G. Pereira. 2021. "Physical Protection of Soil Organic Carbon Through Aggregates in Different Land Use Systems in the Semi-Arid Region of Brazil." *Journal of Arid Environments* 186: 104427.

Monteith, J. L. 1977. "Climate and the Efficiency of Crop Production in Britain." *Philosophical Transactions of the Royal Society of London. B, Biological Sciences* 281, no. 980: 277–294.

Nakhavali, M., R. Lauerwald, P. Regnier, B. Guenet, S. Chadburn, and P. Friedlingstein. 2021. "Leaching of Dissolved Organic Carbon From Mineral Soils Plays a Significant Role in the Terrestrial Carbon Balance." *Global Change Biology* 27, no. 5: 1083–1096.

Nawaz, M. F., G. Bourri, and F. Trolard. 2013. "Soil Compaction Impact and Modelling. A Review." *Agronomy for Sustainable Development* 33, no. 2: 291–309.

Obour, P. B., and C. M. Ugarte. 2021. "A Meta-Analysis of the Impact of Traffic-Induced Compaction on Soil Physical Properties and Grain Yield." *Soil and Tillage Research* 211: 105019.

Oldeman, L. R. 1992. "Global Extent of Soil Degradation." In *Bi-Annual Report 1991–1992/ISRIC*, 19–36. ISRIC.

Or, D., T. Keller, and W. H. Schlesinger. 2021. "Natural and Managed Soil Structure: On the Fragile Scaffolding for Soil Functioning." *Soil and Tillage Research* 208: 104912.

Parton, W. J., A. R. Mosier, D. S. Ojima, et al. 1996. "Generalized Model for N2 and N_2O Production From Nitrification and Denitrification." *Global Biogeochemical Cycles* 10, no. 3: 401–412.

Peng, X., and R. Horn. 2008. "Time-Dependent, Anisotropic Pore Structure and Soil Strength in a 10-Year Period After Intensive Tractor Wheeling Under Conservation and Conventional Tillage." *Journal of Plant Nutrition and Soil Science* 171, no. 6: 936–944.

Poggio, L., L. M. de Sousa, N. H. Batjes, et al. 2021. "SoilGrids 2.0: Producing Soil Information for the Globe With Quantified Spatial Uncertainty." *Soil* 7, no. 1: 217–240. https://doi.org/10.5194/soil-7-217-2021.

Pulido-Moncada, M., S. O. Petersen, and L. J. Munkholm. 2022. "Soil Compaction Raises Nitrous Oxide Emissions in Managed Agroecosystems. A Review." *Agronomy for Sustainable Development* 42, no. 3: 1–26.

Rabot, E., M. Wiesmeier, S. Schlter, and H. Vogel. 2018. "Soil Structure as an Indicator of Soil Functions: A Review." *Geoderma* 314: 122–137.

Romero-Ruiz, A., R. Monaghan, A. Milne, et al. 2023. "Modelling Changes in Soil Structure Caused by Livestock Treading." *Geoderma* 431: 116331. https://doi.org/10.1016/j.geoderma.2023.116331.

Romero-Ruiz, A., D. O'Leary, E. Daly, et al. 2024. "An Agrogeophysical Modelling Framework for the Detection of Soil Compaction Spatial Variability due to Grazing Using Field-Scale Electromagnetic Induction Data." *Soil Use and Management* 40, no. 2: e13039.

Romero-Ruiz, A., M. J. Rivero, A. Milne, et al. 2023. "Grazing Livestock Move by Lévy Walks: Implications for Soil Health and Environment." *Journal of Environmental Management* 345: 118835.

Semenov, M. A., P. D. Jamieson, and P. Martre. 2007. "Deconvoluting Nitrogen Use Efficiency in Wheat: A Simulation Study." *European Journal of Agronomy* 26, no. 3: 283–294.

Shibu, M. E., P. A. Leffelaar, H. van Keulen, and P. K. Aggarwal. 2010. "LINTUL3, a Simulation Model for Nitrogen-Limited Situations: Application to Rice." *European Journal of Agronomy* 32, no. 4: 255–271. https://doi.org/10.1016/j.eja.2010.01.003.

Soares, A., P. Moldrup, A. L. Vendelboe, et al. 2015. "Effects of Soil Compaction and Organic Carbon Content on Preferential Flow in Loamy Field Soils." *Soil Science* 180, no. 1: 10–20.

Steinfeld, H., P. Gerber, T. D. Wassenaar, et al. 2006. *Livestock's Long Shadow: Environmental Issues and Options*. Food and Agriculture Org.

Strock, C. F., H. Rangarajan, C. K. Black, E. D. Schfer, and J. P. Lynch. 2022. "Theoretical Evidence That Root Penetration Ability Interacts With Soil Compaction Regimes to Affect Nitrate Capture." *Annals of Botany* 129, no. 3: 315–330.

Tubeileh, A., V. Groleau-Renaud, S. Plantureux, and A. Guckert. 2003. "Effect of Soil Compaction on Photosynthesis and Carbon Partitioning Within a Maize–Soil System." *Soil and Tillage Research* 71, no. 2: 151–161.

Van Dijk, M., T. Morley, M. L. Rau, and Y. Saghai. 2021. "A Meta-Analysis of Projected Global Food Demand and Population at Risk of Hunger for the Period 2010—2050." *Nature Food* 2, no. 7: 494–501.

van Genuchten, M. T. 1980. "A Closed-Form Equation for Predicting the Hydraulic Conductivity of Unsaturated Soils1." *Soil Science Society of America Journal* 44, no. 5: 892–898.

Vereecken, H., W. Amelung, S. L. Bauke, et al. 2022. "Soil Hydrology in the Earth System." *Nature Reviews Earth & Environment* 3: 573–587.

Wolf, J. 2012. *User Guide for LINTUL4 and LINTUL4V: Simple Generic Model for Simulation of Crop Growth Under Potential, Water Limited and Nitrogen Limited Conditions*. Wageningen University.

Yi, J., W. Hu, M. Beare, et al. 2022. "Treading Compaction During Winter Grazing Can Increase Subsequent Nitrate Leaching by Enhancing Drainage." *Soil and Tillage Research* 221: 105424.

Supporting Information

Additional supporting information can be found online in the Supporting Information section. **Tables S1–S4:** ejss70314-sup-0001-Tables.xlsx. **Table S5:** Summary of all modelling scenarios of this study. All the modelled scenarios comprise 30 compaction simulations (wheel loads of 0.4–12 Mg with 0.4 Mg increments). The *x's* mark the different characteristics of the simulations regarding clay content, mean annual precipitation, mean annual temperature and time until full recovery. The colour code is used in the plots of the results section. **Figure S1:** Summary of the compaction model calibration using soil bulk density data from a soil compaction experiment in Zürich, Switzerland (Keller et al. 2017). The model parameters were calibrated to fit soil bulk density data after compaction as a function of soil depth (a). The normal stress profile inferred by the compaction model and the measured stress (b), the modelled macroporosity before and after compaction (c) and the modelled saturated hydraulic conductivity before and after compaction (d). Simulated changes in bulk density at 10 cm depth as a function of wheel load (e) based on the calibration presented in (a). **Figure S2:** Mean annual precipitation (a) and temperature (b) for the 50 years simulated in this study and different precipitation and temperature regimes. (c) Mean daily temperature as a function of the day of the year for all 50 simulated years. **Figure S3:** Means of the van Genuchten (1980) model parameters and Ksm as a function of the mean clay content (crosses), as reported by Carsel and Parrish (1988), with their respective regression curves (solid lines). The figure shows residual water content (a), saturated water content (b), the empirical parameters alpha (c) and *n* (d) and saturated hydraulic conductivity of the soil matrix (e). **Figure S4:** Modelling results comparing relative impacts of soil compaction on crop yield (accumulated in 20 years after initial compaction) (a), soil organic carbon stocks (at year 20 after initial compaction) (b), nitrous oxide emissions (accumulated in 20 years after initial compaction) (c) and nitrate leaching (accumulated in 20 years after initial compaction) (d) for different wheel loads and fertilisation rate. **Figure S5:** Modelling results comparing relative impacts of soil compaction on crop yield (accumulated in 20 years after initial compaction) (a), soil organic carbon (at year 20 after initial compaction) (b), nitrous oxide emissions (accumulated in 20 years after initial compaction) (c) and nitrate leaching (accumulated in 20 years after initial compaction) (d) for different levels of compaction represented as increasing bulk density. These modelling results show differences between different clay contents. **Figure S6:** Modelling results comparing absolute impacts of soil compaction on crop yield (accumulated in 20 years after initial compaction) (a), soil organic carbon stocks (at year 20 after initial compaction) (b), nitrous oxide emissions (accumulated in 20 years after initial compaction) (c) and nitrate leaching (accumulated in 20 years after initial compaction) (d) for different levels of compaction represented as increasing bulk density. These modelling results show differences between different clay contents. **Figure S7:** Modelling results comparing relative impacts of soil compaction on crop yield (accumulated in 20 years after initial compaction) (a), soil organic carbon stocks (at year 20 after initial compaction) (b), nitrous oxide emissions (accumulated in 20 years after initial compaction) (c) and nitrate leaching (accumulated in 20 years after initial compaction) (d) for different levels of compaction represented as increasing bulk density. These modelling results show differences between different mean annual precipitation. **Figure S8:** Modelling results comparing relative impacts of soil compaction on crop yield (accumulated in 20 years after initial compaction) (a), soil organic carbon stocks (at year 20 after initial compaction) (b), nitrous oxide emissions (accumulated in 20 years after initial compaction) (c) and nitrate leaching (accumulated in 20 years after initial compaction) (d) for different levels of compaction represented as increasing bulk density. These modelling results show differences between different mean annual temperatures. **Figure S9:** Modelling results comparing relative impacts of soil compaction on crop yield (accumulated in 20 years after initial compaction) (a), soil organic carbon stocks (at year 20 after initial compaction) (b), nitrous oxide emissions(accumulated in 20 years after initial compaction) (c) and nitrate leaching (accumulated in 20 years after initial compaction) (d) for different levels of compaction represented as increasing bulk density. These modelling results show differences between different recovery rates. **Figure S10:** Modelling results of texture-scenarios comparing relative impacts of soil compaction on crossplot of crop yield and carbon stocks (a), yield and yearly nitrate leaching (b) and yearly nitrous oxide emissions (c) and yearly nitrate leaching (d). Each modelled point corresponds to all levels of compaction on a given year for the first 50 years after compaction. **Figure S11:** Modelling results comparing relative impacts of soil compaction on relative WFPS for different clay content (a), precipitation (b), precipitation (c) and recovery rates (d). The control line (no compaction = 1). **Figure S12:** Modelling results comparing relative impacts of soil compaction on the transpiration reduction factor (soil water related) for biomass formation for different clay content (a), precipitation (b), precipitation (c) and recovery rates (d). The control line indicates no compaction (no compaction = 1). **Figure S13:** Modelling results comparing relative impacts of soil compaction on soil organic carbon inputs from death roots and straw (a), root length as a function of soil depth (b), soil organic carbon losses due to CO_2 emissions (c). **Figure S14:** Modelling results comparing relative impacts of soil compaction on soil organic carbon stocks as a function of soil depth for different clay content (a), mean annual precipitation (b), mean annual temperature (c) and recovery rate (d). **Figure S15:** Modelling results comparing relative impacts of soil compaction on air filled pore space (AFPS) for different clay content (a), mean annual precipitation (b), mean annual temperature (c) and recovery rate (d). The control line indicates no compaction (no compaction = 1).